Membrane and Arrayed Nanofluidic Devices with High Density Aligned Carbon Nanotubes

by

Samaneh Shadmehr

A thesis

presented to the University of Waterloo

in fulfillment of the

thesis requirement for the degree of

Doctor of Philosophy

in

Chemistry (Nanotechnology)

Waterloo, Ontario, Canada, 2015

AUTHOR'S DECLARATION

I hereby declare that I am the sole author of this thesis. This is a true copy of the thesis, including any required final revisions, as accepted by my examiners.

I understand that my thesis may be made electronically available to the public.

Abstract

Exceptionally high aspect ratio, smooth hydrophobic graphitic walls, and nanoscale inner diameters of carbon nanotubes (CNTs) cause the unique phenomenon of efficient transport of water and gas through these nanoscale molecular tubes. Molecular transport through the cores of CNTs is of significant interest from both fundamental and application aspects. The application of CNTs as nanofluidic channels is envisioned in many areas, ranging from desalination, carbon capture, drug delivery, DNA sequencing and translocation, protein separation, single molecule sensing, to nanofluidic transistors and diodes. A fundamental understanding of the mechanisms governing molecular transport through CNT pores is much needed and, unfortunately, still lacking, which demands further research. In this work, CNT-based smart membranes and arrayed devices are explored both as a versatile platform for fundamental studies and as exemplary devices for biosensing applications.

In Chapter 3, a study of ion transport across smart, DNA-functionalized CNT membranes is reported. The diffusive transport rates of ferricyanide ions were monitored through an array of vertically aligned CNTs (VA-CNTs) functionalized with amine-modified single-stranded DNA (ssDNA) (Cy3-T15-NH2) probes. Reversible closing of CNT pores was achieved by the addition of complementary DNA (A15), gating ion transport. Our analysis suggests that pore blocking occurs due to steric hindrance at the CNT pore entrances.

Chapter 4 focuses on the design and fabrication of arrayed CNT devices. Each device consists of a large number (roughly $4x10^5$) of aligned multiwalled CNTs span a barrier separating two fluid reservoirs, enabling direct electrical chronoamperometric measurement of ion transport through the nanotubes and analyzing ion transport properties. Here we intend to demonstrate the theoretically predicted ultrahigh ion flow rate through multiplexed CNT devices that are directly electrically addressable. Compared with traditional nanopore devices, ours feature distinct advantages. The CNTs have a remarkably high aspect ratio and they can confine an entire molecule and also extend the duration of transport, which is likely to result in new translocation characteristics. Our devices have a planar design, which enable simultaneous optical and electrical probing.

Results presented in this work show the potential of CNT nanofluidic devices for the fundamental studies of the nanoconfinement effects on ion transport. The developed synthesis and fabrication methods are envisioned to lead to novel biosensors based on nanofluidics, which can find a broad spectrum of significant applications such as disease diagnostics, food safety monitoring, and environmental pollution detection.

Acknowledgements

I would like to thank my supervisor, Dr. Shirley Tang for her invaluable guidance and support during my PhD. My sincere thanks to my committee members, Dr. Tong Leung, Dr. Dan Thomas, and Dr. Frank Gu for their encouragement and their insightful comments to improve my thesis. I would like to express my appreciation and thanks to Dr. Suresh Neethirajan for his valuable comments and suggestions on my thesis. Thanks to the past and current members of Dr. Tang's group: Dr. Himadri Mandal, Dr. David Donkor, Dr. Mahyar Mazloumi, Yverick Rangom, Xiguang Gao, Andrew Ward and Mike Coleman.

I would like to acknowledge the support of Dr. Raafat Mansour, the director of center for Integrated RF Engineering (CIRFE) at University of Waterloo for providing me the opportunity of working in the CIRFE clean room facility. I would also like to thank all my supportive colleagues at CIRFE, especially Dr. Salam Gabran for always being helpful. My thanks to Dr. Juewen Liu and his PhD student, Biwu Liu for their valuable comments.

I would like to express my gratitude and thank to my lovely friends: Bahareh, Elnaz, Fahimeh, Golnaz, Leyla, Mona, Nafiseh, Raheleh, Sepideh, Sevda and Zhaleh who showed me the real meaning of friendship. Thanks for being what you are.

I would like to express my deepest gratitude to my adorable parents, brothers and parents-in-law for their continuous love and everlasting support, even from thousands of miles away. It is hard to believe that I could survive these years far from you.

The last but not the least, I would like to give my heartfelt thanks to you, Behrooz, for your unconditional love, support and inspiration during this journey and for trusting me in reaching my dreams.

Dedication

To Behrooz, Maman and Baba,

with whom I experienced pure love.

Table of Contents

List of Figures

List of Tables

Chapter 1: Introduction and Thesis Objectives

1.1 Introduction to Carbon Nanotubes and their Applications

Nanotechnology is having a profound impact on our society. The global earnings of businesses incorporating nanotechnology hit $254 billion in 2009[1]. The invention of new functional nanomaterials and nanodevices has greatly improved our lives. Nanotechnology involves the synthesis and fabrication of material at sizes of less than 100 nm, and improves production using more efficient and sustainable ways. For instance, Carbon nanotube (CNT) is one of the greatest discoveries[2]. CNTs are an allotrope of carbon, in addition to diamond and graphite, and have a range of electrical, thermal, and structural properties that can change based on the physical design of the nanotube.

Carbon structures can be classified based on the nature of their carbon-carbon bonds. In diamond, chemical bonding occurs as a result of sp^3 hybridization in a tetrahedral lattice pattern. In graphite, carbon atoms sp^2-hybridize to form a hexagonal lattice in two-dimensional layers named graphene, which are arranged on top of each other and held by weak van der Waals forces. Carbon in sp^2 hybridization can form other exciting structures, like the cylindrical form seen in CNTs. In 1991, Ijima first discovered graphitic shells with an inter-layer separation of ~0.34 nm, diameters of ~10 nm, and a high length-to-diameter ratio. These are now known as multi-walled carbon nanotubes (MWNTs)[1]. In 1993, Ijima et al. discovered single-walled carbon nanotube (SWNT)[3], which consists of a graphene sheet rolled into a cylindrical tube. The diameter of a SWNT is on the order of one nanometer,

about 5 x 10^4 times smaller than the thickness of a human hair, whereas the length of a SWNT can be up to several millimeters. Therefore, a CNT can have an aspect ratio (length-to-diameter ratio) of up to 10^8:1, which is considerably larger than that of any other material[4].

1.1.1 Extraordinary properties of CNT

CNTs exhibit extraordinary mechanical, thermal and electrical properties. The elastic modulus of SWNT is about 1000 Gpa (1 TPa), which is five times higher than the strength of carbon steel[5]. Theoretically, the thermal conductivity of SWNT is up to 6600 W/ (m K), more than five times higher than that of diamonds. Due to the elimination of electron scattering, CNTs can be ballistic conductors. They have the highest current density (109 A/cm^2) on record, which is 100 times greater than that of copper wires[6]. The high aspect ratio (up to 1.36×10^8) and surface area (up to 1315 m^2/g) offer a high surface area for modification of CNTs with functional molecules[7,8].

The unique structure of CNT contributes to the distinguishing thermal and electrical properties that make them potentially useful in a wide range of applications in electronics and optics. In particular, CNTs have been explored as the main components of energy transport in next-generation devices such as light-emitting diode (LED), field-effect transistor (FET), thermal rectifier, and photon wave-guide[9] due to their axial electrical conductivity[10,11] and thermal conductivity[12–14] in high aspect ratio[15,16]. In addition, CNTs possess atomically smooth surfaces[17], and researchers have proposed CNTs as ideal candidates for mass transport in nanoscale, such as molecular transport, selective gas permeation, and nanofluidics.

1.1.2 CNT Basic Structure

CNTs are the tubular allotrope of carbon with sp^2 hybrid C=C bonds. As mentioned, they can be formed as single walled (SWNT), double walled (DWNT), or multi walled (MWNT) concentric tubes. Figure 1-1 shows the structure of CNTs. Additionally, they can have different chiralities, diameters, lengths, and they can be organized into films, mats, forests, and yarns[18–21]. Figure 1-1a shows a TEM image of a DWNT and a MWNT with different diameters and number of walls. Figure 1-1b shows schematically the hexagonal order of the carbon atoms in the graphene sheet. The direction and vector around which the graphene sheet rolls determines the chirality of the obtained CNT.

Basically SWNTs are described with a vector called the chiral vector, $\vec{C}$, which is defined as follows:

$$\vec{C} = n\overrightarrow{a_1} + m\overrightarrow{a_2} \qquad (1.1)$$

in which n and m are integers and $\overrightarrow{a_1}$and $\overrightarrow{a_2}$ are the unit cell vectors in the two-dimensional lattice of the graphene sheet[22]. The nanotube axis is perpendicular to the chiral vector $\vec{C}$. The value of (n,m) defines the chirality of the nanotubes (i.e., armchair, zigzag and chiral) and its electrical, optical, thermal and mechanical properties.

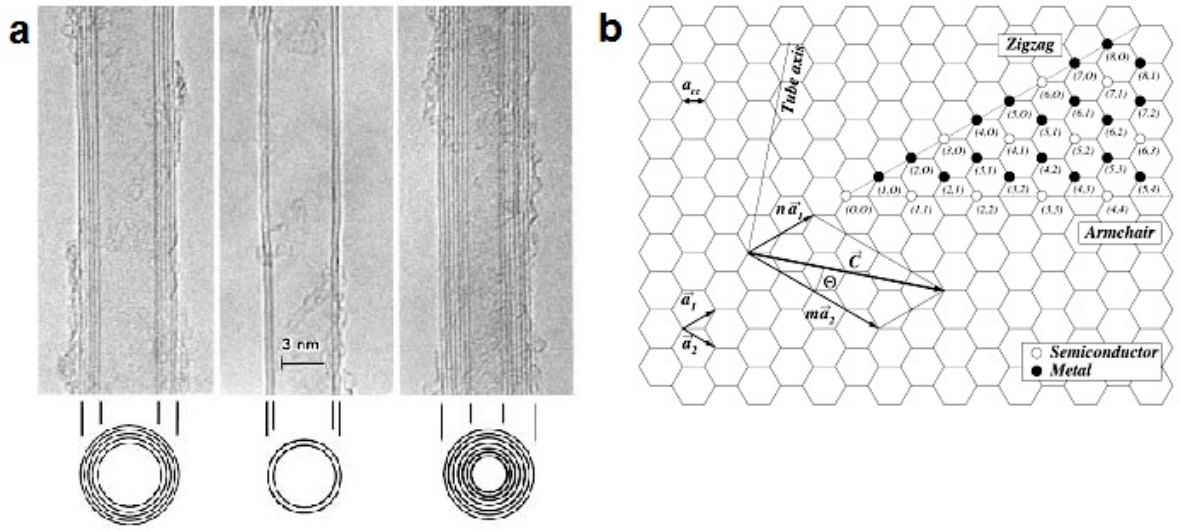

Figure 1-1: TEM and representative images of carbon nanotubes. (a) TEM images of double walled and multi walled CNTs (by Iijima, 1991[2]). (b) Schematic drawing of a hexagonal lattice of carbon atoms showing the chiral vector $\vec{C}$ and chiral angle θ for a (2,4) nanotube (by Avouris et al., 2001[4], Reprint with permission).

For instance if |n-m|=3p, the nanotubes are metallic (highly conducting), and if |n-m|=3p±1, the nanotubes are semiconducting (p is an integer). The diameter of the nanotubes can be obtained by the following formula:

$$d = 0.344 + 0.1\exp\left(-\frac{c}{4\pi}\right) \qquad (1.2)$$

in which $\frac{c}{4\pi}$ is the radius of the tube and c is the length of the chiral vector $\vec{C}$ and is equal to the circumference of the nanotube[22]:

$$c = |\vec{c}| = a\sqrt{n^2 + nm + m^2} \qquad (1.3)$$

Multi walled CNTs (MWNTs) are tubular structures with several concentric SWNTs, as shown in TEM images. Their electronic properties are not as diverse as those of SWNTs, and they are mostly metallic[23].

1.1.3 Synthesis of CNTs

1.1.3.1 Chemical Vapor Deposition

There are different methods of synthesizing CNT, including arc discharge, laser ablation, high-pressure carbon monoxide (HiPCO), and chemical vapor deposition (CVD)[24,25]. Of these, CVD is the most widely used method for creating controlled CNT structures, because it allows for a relatively desirable yield, and can be used to produce vertically aligned, rather than randomly oriented, CNTs with few defects (Figure 1-2)[26]. CVD takes a bottom-up approach, in which the 'root' catalysts of metal-nanoparticles are exposed to carbon sources at a high temperature to give rise to CNT. First, a substrate is prepared with a layer of metal catalyst particles, such as nickel, cobalt, iron, or a combination of these, and is heated to approximately 700 °C[26]. Then, two kinds of gases are introduced into the reactor: process gases, such as ammonia, argon, and nitrogen, which constitute the surrounding atmosphere, and an actual hydrocarbon source, such as acetylene, ethylene, ethanol or methane. Subsequently, in a process called pyrolysis, the hydrocarbon from the source is decomposed by plasma or thermally and becomes in contact with metal catalysts to initiate the growth of CNTs.

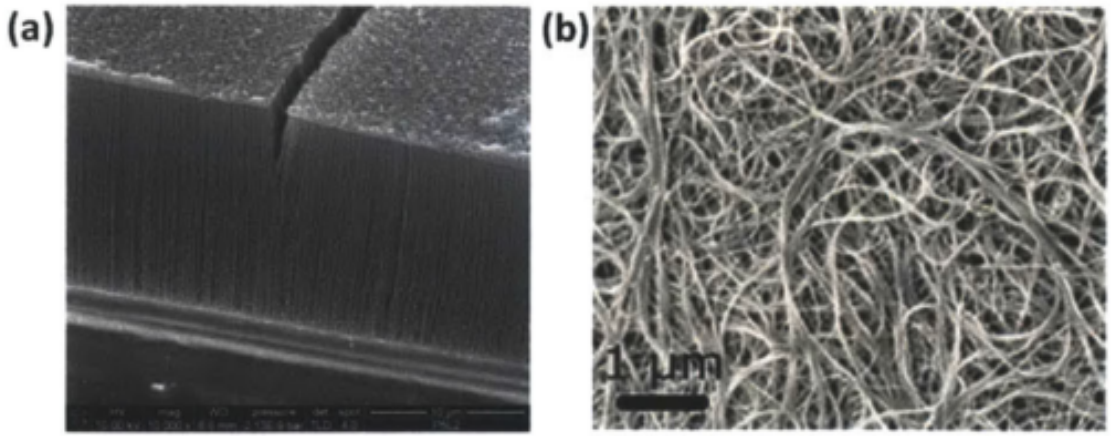

Figure 1-2: Comparison of CNTs grown by CVD and other methods. (a) Highly, vertically aligned SWNTs fabricated by CVD. (b) Unaligned, mixed SWNTs produced by arc discharge.

In 2006, Brukh and Mitra studied CVD reaction pathways, with C_2H_4 as the carbon precursor[27]. It is now commonly accepted that ethylene goes through the following reactions to produce elemental carbon. First, C_2H_4 decomposes to form acetylene (C_2H_2) via:

$$C_2H_4\,(g) \rightarrow C_2H_2\,(g) + H_2\,(g) \qquad (1.4)$$

The Acetylene then reacts with hydrogen radical (H) to form a vinyl radical (CH_3) and elemental carbon (C), which will produce either CNTs or non-tubular carbon:

$$C_2H_2\,(g) + H\,(g) \rightarrow CH_3\,(g) + C\,(g) \qquad (1.5)$$

It is important to note that the identity of the CNT formed does not solely depend on the nature of the hydrocarbon source, but also on other parameters, such as the properties and composition of the metal catalyst, metal-support interactions, and reaction conditions like

temperature, pressure, inert/hydrocarbon gas ratio and gas flow rate[26]. With present technology, researchers have limited control of the parameters, making it difficult to synthesize one specific type of CNT. Thus, a proper identification or separation process is often implemented to extract the target CNT from as-synthesized CNTs.

1.1.3.2 Synthesis of Aligned CNT Structures

In early 1990s, researchers tried to synthesize carbon nanostructures on a large scale for industrial use. They also attempted to fabricate controlled structures of aligned CNTs. At this stage research was done to explore the electrical, optical and magnetic properties of CNTs. One of the applications for the aligned nanotubes is to fabricate field-emission devices. In 1995, a French group, reported the fabrication of aligned MWNT films by arc evaporation process[28]. Consequently, other research groups synthesized aligned CNT patterns using other techniques. Compared with other techniques, CVD is the most scalable and industrially feasible process for the synthesis of CNTs. Vertically aligned CNT (VA-CNT) films have been grown on a substrate having iron nanoparticles as catalysts incorporated in a silica matrix[29]. In 1998, Ren et al. studied the synthesis of aligned MWNTs on nickel coated glass substrates by plasma enhanced, hot filament, chemical vapor deposition from a combination of acetylene and ammonia[30]. However, in this case, significant portion of the CNTs had bamboo like structures due to the low temperature formation. Likewise, another group of researchers produced aligned CNT arrays using hydrocarbons and ferrocene as catalysts[31]. Researchers at the University of Kentucky have concentrated on improving and high-scale fabrication of MWNT arrays by using ferrocene

and xylene at about 650 ºC[32]. The catalyst decomposes to make particles, which are deposited on the substrate. The carbon sources then react with the catalyst and eventually crystalline graphite walls grew on the catalyst nanoparticles. Therefore, the dimension of the catalyst particle defines the diameter of the CNTs. The carbon nanotubes grow by a combination of tip and base growth mechanisms, with the catalyst nanoparticle detected at the top of some growing CNTs[33].

One of the approaches for alignment of CNTs, for the application of some partial alignment of CNTs in a polymer matrix, was done by mechanical stretching[34]. These nanostructures could also be aligned along the flow direction throughout extrusion of a polymer composite melt[34]. Alignment of CNTs can also be accomplished by extruding a polymer melt of polystyrene and nanotubes in the direction of the extrusion[35]. For the samples that have a large volume of CNTs, we cannot have a great alignment, because the melt is not fluid enough. A research group at Rice University could align SWNT bundles by applying a magnetic field of about 7 T during the filtration of CNT suspension filtration process[36,37].

1.1.4 Patterned Aligned CNT Structures

Owing to the advances in Micro and Nanotechnology, several fabrication techniques have been developed to use the patterning processes in designing various catalyst configurations and shapes on substrates. Photolithography is a technique in which a substrate with a desired pattern design is made, on which a catalyst thin film can later be deposited.

The patterned catalyst, when used for CNT growth, results in a patterned CNT structure with a three-dimensional configuration.

Basically, the substrate is coated with a light-sensitive chemical called “photo-resist”, or simply “resist”. Later, a light source (UV for example) is used to transfer a geometric pattern from a photo-mask to the photo-resist coated on the substrate. Then the exposed area is treated chemically, either to stabilize or fix the patterned design on the photo-resist or to etch it away, depending on the photo-resist type (i.e., negative or positive, respectively, Figure 1-3). Figure 1-3 shows photolithography procedure by using lift-off resist (LOR) or Polymethylglutarimide (PMGI) resist.

The pattern obtained on the substrate can be coated with a metal catalyst through electron beam deposition or sputtering techniques (step 5). At the end, when the photo-resist has been removed in the lift-off step, the patterned designs of the desired metallic catalyst remain on the substrate. The substrate obtained with the patterned catalyst design can be used to grow CNTs through a CVD process. Various patterns of the aligned CNTs can be grown by this method on a patterned design of Fe catalysts on a Si/SiO_2 substrate. During the growth in the CVD chamber and at high temperature, growth gases dissociate on the catalyst patterns on the substrate, dissolve in it, and later CNTs grow only at those areas where catalyst film is present. Therefore, several different patterns of aligned CNTs can be made with this technique, which can be beneficial for diverse applications.

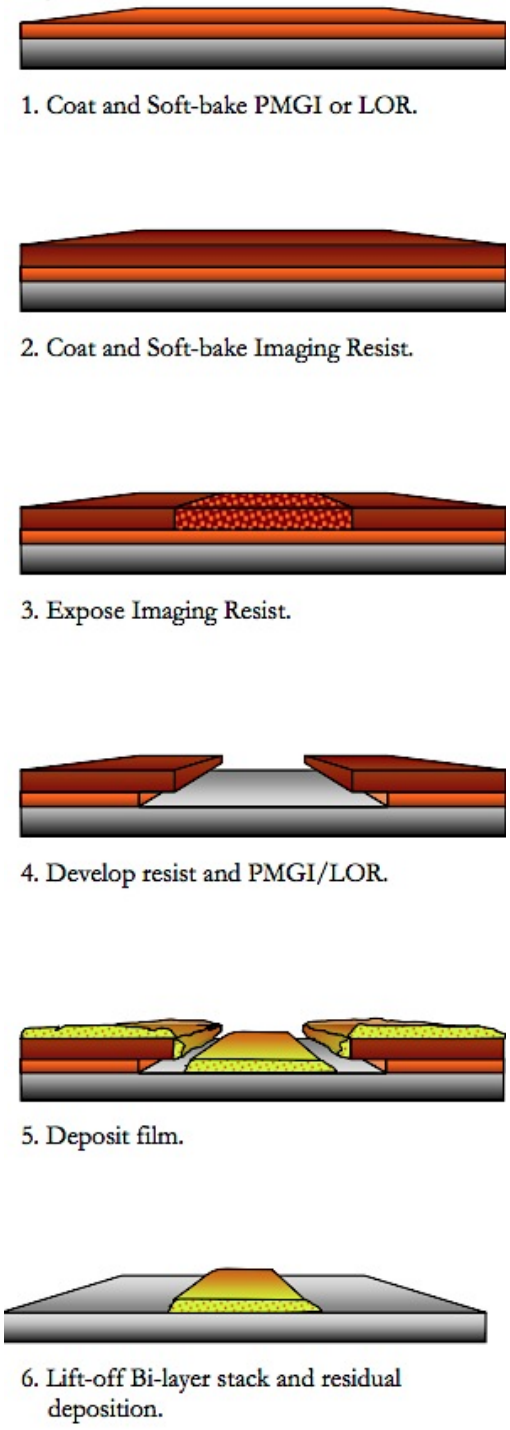

Figure 1-3: Photolithography process with lift-off resist (MicroChem, USA)

Using CVD method, improvements have been done to reduce the production of amorphous carbon on the catalyst particles and therefore increase the growth yield of nanotubes[20,21]. It has been shown that small amounts of water vapor or oxygen together with the synthesis gases can reactivate the catalysts and therefore, longer CNTs can be obtained[21,38]. At growth temperatures, catalyst thin films turn to nanoparticulate islands, i.e. catalyst nanoparticles, dispersed homogenously all over the substrate. The density and size of the catalyst nanoparticles depend on the thin film thickness and the annealing temperature, and therefore define the final morphology of the CNTs. The more dense the catalyst dispersion, the more compact the CNT structure, because the nanotubes lean on each other when they are growing as a result of van der Waals forces[39]. Wei et al.[39] have shown that the thinner the catalyst film, the smaller the particles are during thermal annealing, and the denser are the obtained CNTs.

It has been reported that the presence of a thin alumina supporting layer enhances the catalyst activity and density of the CNTs as well as their length, and these features are influenced by the porosity of the alumina layer[40]. It is possible to grow CNTs as tall as a few millimeters with the help of an alumina supporting layer[41].

1.2 Membranes with VA-CNTs

1.2.1 What Are Membranes

A membrane is a continuous 2 dimentional material (e.g. graphitic sheet) base on a physical chemistry definition. From a biological perspective, it is a lipid film having highly selective protein channels. In this thesis, membranes are defined as 2D films that allow

selective transport driven by forces, such as concentration, pressure, or electric field gradient. The main application of a membrane is to transport specific specie over other kinds. For instance, a reverse-osmosis membrane is a polymer film that permits water to pass through but salt to be preserved, and can be used to desalinate salty water. A microfiltration membrane will preserve colloidal particles and can be applied for drinking water filtration. Different factors, such as size exclusion in porous membranes, diffusivity in polymeric membranes, and electrostatic forces in nanofiltration, are functioning in combination with one another.

Understanding transport phenomena at the nanoscale is an important challenge, because it consists of chemical, electrical and mechanical effects. Membranes with pores that are uniform and well defined are platforms of interest for basic investigation of membrane transport. Such membrane structures are promising for simultaneous flux and selectivity increase.

1.2.2 Fabrication of VA-CNT Membranes

The membrane fabrication process is to use grown crystalline CNTs and to seal the space between the CNTs by using a polymer matrix[42] or ceramic as filler[43] while preserving the CNTs alignment, and using plasma oxidation in order to open up the CNTs. Researchers at the University of Kentucky fabricated the first VA-CNT membrane in a polymer. The membranes consisted of about 1010 CNTs/cm^2, with dimensions of about 7 nm, and which allowed measurement of transport of gases and ions through these membranes[42].

As this thesis is on a membrane structure, which is composed of CNTs in a polymer matrix, a short paragraph on polymer nanocomposites is presented. Polymer nanocomposites are described as the combination of a polymer matrix and attachments that have at least one dimension in the nanometer range. CNTs are nanomaterials with their diameters in the nanoscale and have remarkably high mechanical potency, electrical conductivity, and high aspect ratio, making them great candidates to add in polymer matrices[44]. Randomly oriented CNTs have been used as supports on polymers like poly-vinyl alcohol[45], and polystyrene[46]. Aligned CNT polymer composites are interesting structures for applications such as field emission devices, electromagnetic protecting devices[47] and also for membranes[42]. Ravarikar et al[48] published an article reviewing the mechanism of infiltration of methyl acrylate monomers in MWNT arrays and it's following polymerization. Another example is polystyrene that has high wettability[49] with CNTs and so fabrication of a film by a spin coating method is straightforward.

The vertically aligned CNTs in the polymer matrix frequently have a graphitic cap or the catalyst metal particle closing the graphitic cores. In order for the vertically oriented membrane structure to have the nanotubes as transporting channels, these materials need to be removed. Liming Dai et al.[50] have showed the possibility of applying the plasma oxidation process to eliminate amorphous carbon layers and open CNTs without destroying their structure. Some oxidation methods, including high temperature treatment[51] or harsh acid treatment would destroy the membrane. Plasma-oxidation process is efficient because its controllable, and it's possible to fabricate a macroscopic CNT array device. The plasma-

oxidation process which is a key step for membrane fabrication, acts three important functions: It removes residual polymers and expose the CNT tips out of the polymer matrix by oxidative etching, as the oxidation kinetics of the polymer is faster than that of the CNTs; It etches amorphous carbon and Fe impurity by HCl treatment; Finally, it introduces functional groups (–COOH) at the CNT tips, which makes the tips ready for chemical functionalization. The CNT membrane structure reported by the Hinds group, showed a BET pore-size distribution of about 6 ±2 nm, after the plasma oxidation process, which is in agreement with TEM observations of the inner core of about 7 nm[42]. A schematic of the membrane fabrication process is indicated in Figure 1-4. The CNT membrane demonstrated transport of gases and ions, which shows that the above process is capable of forming a practical membrane structure, composed of vertically aligned open CNTs, which function as channels for molecular transport.

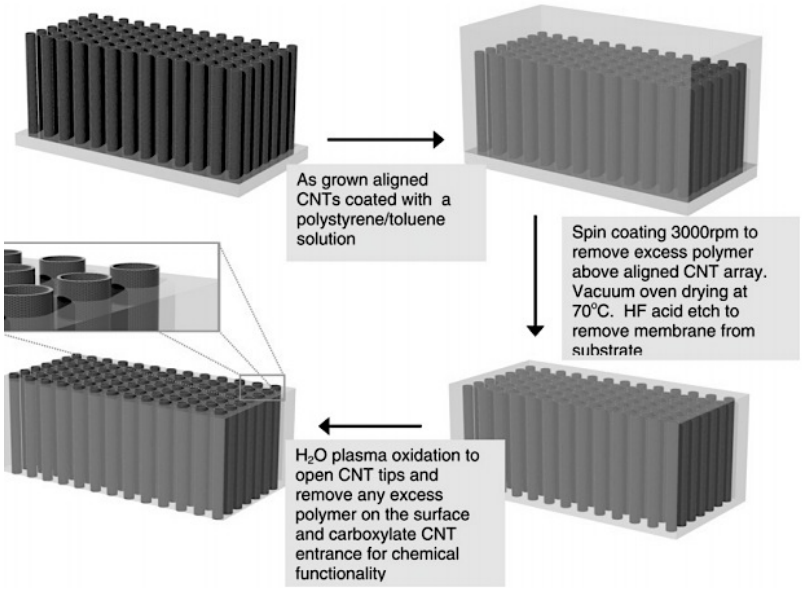

Figure 1-4: Processing steps involved in aligned CNT membrane fabrication process. with permission from reference[52].

1.3 CNT Nanofluidics

CNTs, with nanometer scale diameters and smooth surfaces, offer a unique system for studying molecular transport and nanofluidics. Although the idea that water can occupy such confined hydrophobic channels is somewhat counter-intuitive, experimental evidence has verified that water can actually occupy these channels[53,54]. Water transport through molecular-scale hydrophobic channels is also important because of the similarity of this system to transmembrane protein pores[55,56]. In recent years, numerous simulations[57,58] of water transport through SWNTs have proposed that water can occupy these nanochannels, and furthermore fast molecular transport happen. Molecular dynamics (MD) simulations suggest that the increase in molecular transport relates to the smoothness of the nanotube

inner core and also relates to molecular ordering phenomena that may happen in the CNTs with an inner diameter of 1 to 2 nm[57–59]. For similar reasons, simulations of gas transport through SWNTs[60] predict flux enhancements of several orders of magnitude relative to other similarly sized nanoporous materials. Membrane-based gas separation systems using zeolites provide precise separation and size exclusion, although often at the expense of throughput or flux. It may be possible to use SWNT to create a membrane that offers both high selectivity and high flux.

Considering such theoretical predictions, it is essential to verify the fast transport phenomena experimentally. The unique geometry of the CNT allows chemical modifications to be placed specifically at the pore openings, allowing for gatekeeper activity. The term "gate keeper" is used here to refer to a chemical layer only at the pore entrances that selectively allows chemicals to pass into and through the pores of the membrane, much like how natural protein channels work. Both enhanced transport and gatekeeper selectivity are key elements for mimicking natural protein channels. Success with this approach would allow for fast transport and high selectivity, which is not attainable with conventional membrane systems to match the performance level of natural protein channels. Researchers have recently fabricated MWNT-membranes with larger pore diameters (6 to 7 nm) by encapsulating vertically aligned arrays of MWNTs within polymer matrices[42,43] and by templated growth within nanochannels[61]. Enhanced water transport through these larger MWNTs has recently been reported[62]. Quantifying transport through an individual tube in a MWNT membrane is difficult because MWNTs are prone to blockages, in particular by

"bamboo" structures and catalyst particles that can migrate to and obstruct the nanotube interior[63–65]. The consequence of such blockages is a marked reduction of the active membrane pore density. In contrast, there are few reports of "bamboo" structure formation or catalyst migration in SWNTs or double-walled CNTs (DWNTs). However, it has been difficult to produce VA-CNTs uniformly and at large scale[38,58]. The main challenges are in defining a deposition procedure to seal the gaps in the nanotube array and moreover in performing a selective etching procedure to open the nanotubes without creating holes in the membrane structure. The technical challenges in nanofabrication are some of the key causes for the difference between the amount of studies from computational and experimental reports, and they offer great research opportunities in experimental CNT nanofluidics.

1.4 Thesis Motivation and Objectives

This Ph.D. thesis focuses on comprehending the molecular transport properties through CNTs. Significant to the study is the design of a CNT membrane structure, which contains a considerably large number of vertically aligned CNTs (about $10^{10}/cm^2$) letting macroscopic measurement of transport across the CNT membrane. The principal goals of the thesis are to develop a new platform by which to realize and study ion transport through the atomically smooth CNT cores, to verify that charged molecules attached to the conducting CNT membranes control the molecular transport, and to indicate the potential of the CNT nanofluidic devices for the fundamental studies of ion transport. We also aim to develop synthesis and fabrication techniques to design and fabricate novel biosensors based on CNT nanofluidics, which have various significant applications in health and environment.

Chapter 2: CNT Nanofluidics

Recent developments in nanotechnology have facilitated the combination of nanomaterials and conventional microstructures, and so the monitoring of the nanoscale behavior of mass transport or fluid dynamics of molecules or ions enclosed in geometries comparable with molecular dimension. Here, we introduce and provide a summary and overview of CNT Nanofluidics. CNT Nanofluidics is a field of study and a research area that conveys mass transport through CNTs under nanoscale confinement.

The following sections explain recent accomplishments done by experimental and theoretical research groups aiming for the kinetics of ions in CNTs, including transport of ions under CNT nanoconfinement, selectivity and ion exclusion in connection with CNT-based membrane skill. Lastly, this section concludes with some aspects of CNT Nanofluidics.

2.1 CNTs as Nano-vessels or Mass Transport Nanochannels

In 1993 Ajayan and Ijima[66] for the first time performed the viability of liquids infiltrating the cores of CNTs and acting as nanocontainers. In a following publication by the same group, it was reported that, comparing metals, inorganic materials were difficult to diffuse inside open CNTs[67]. This is because inorganic materials have higher surface energy mismatch with the CNT compared with liquid metals. The significant outcome of this study was the possibility of opening the CNTs using gas phase oxidation. One of the applications of such penetration performance is the template assisted synthesis of nanomaterials[68].

In 1994 and 1998, Dujardin et al.[69] studied the wetting behavior of CNTs and reported the results. In their experiments molten metals were infiltrated in MWNT samples with diameters of 2 to 20 nm and they concluded that some liquids with a surface tension of less than 180 mN/m would wet the MWNTs. Therefore, liquids like water could easily wet the MWNT, but not for all molten metals. A following study demonstrated that SWNT samples perform similarly.

CNTs as nanochannels for molecular transport study have interested scientists and engineers. Some research groups started investigating on the unique transport properties of CNTs and this was possible due to the rapid improvement and progress of molecular simulation methods. David Sholl and Karl Johnson at Carnegie Melon University studied the diffusion of gases like Ar, N_2, and CH_4, through nanoporous materials including CNTs. The inspiration for their findings was to study some potential inorganic materials for gas separation applications. This group reported that the transport of argon gas through CNT membranes were approximately 3 to 4 orders of magnitude more than through zeolitic pores[59]. They reported that the reason for the enhanced transport through CNT membranes is the smooth and frictionless graphitic CNT walls that allow specular reflection of the gases. Another study has been done by the Susan Sinnot group at the University of Kentucky[70] on gas transport through CNTs using molecular dynamics. Their simulation studies also predicted very fast transport of gases through CNTs[71].

Nick Quirke's group at Imperial College explored the hydrodynamics of fluid flow for low Knudsen number fluids through graphitic pores. Their studies indicated that there is

large slip lengths for these fluids[72]. For the first time, in 2002, they suggested the existence of slip boundary conditions on smooth CNT surfaces[73]. The same research group reported extremely rapid diffusion of oil in CNTs which is not understandable by the Washburn equation[57].

Gerard Hummer and his team at the National Institute of Health in Maryland were interested in studying water transport through CNTs and this was mainly inspired by the tubes' hydrophobic nature and resemblance to protein channels. Molecular Dynamics simulations compared CNTs to the protein channels. CNTs offered a much simpler model for their important publication in 2001. The authors suggested that water transport through hydrophobic CNT channels occurs at an peculiar speed through the supportive movement of a hydrogen bonded network through the smooth walls of CNTs[58]. Kalra et al.[74] investigated the osmotic transport of water through CNTs. The studied water flow velocities were similar to he ones realized in natural water channels like aquaporin. Klaus Schulten's group also studied the water and proton transport performance through CNTs. The water dipoles were highly aligned unidirectional in original nanotubes. This alignment was slightly disturbed in the modified CNTs[75]. More simulation studies by other groups will be mentioned in subsequent sections, specifically the ones related to the experimental studies in this thesis.

Another research group studied the transport of liquids in SWNT bundles. Their observation of induced voltage in the direction of flow was not consistent with standard electrokinetic phenomena and was described by an induced charge mechanism at the

polarizable liquid electrolyte interface[76]. The observed voltage is a function of the liquid ionic properties and so this device could be used as a flow sensor.

Gogotsi et al. of Drexel University have studied the behavior of water inside hydrothermally synthesized CNTs by *in situ* microscopy techniques. In 2002,[53] the research group reported the flow velocities of water to be about $0.5x10^{-4}$ cm/s in nanotubes with 50 nm inner diameter. This research group also studied the kinetics of water inside disordered carbon nanotubes, Appling scanning electron microscope. In the current work, the CNTs were occupied with water, then frozen at -80 ºC and analyzed by HR-TEM and EELS[77]. Based on the observations from these experiments, it was found that there was a segmented filling of water with air bubbles inside CNTs with pore diameter of about 20 to 100 nm and a thorough filling for the pore diameters of 5 to 10 nm. For the case of crystalline nanotubes a gap of about 4 Å was observed in between the graphitic walls and the frozen water[78]. This finding proposes that water molecules did not wet crystalline CNTs with small diameter.

The first experimental mass transport measurements of CNTs was performed on single pore carbon nanotube membranes with about 120 nm pore diameter[77]. This large diameter nanotube did not demonstrate any unusual transport properties and was synthesized for Coulter counting applications. A Coulter counter is a device that can calculate biological cells or particles. The single pore device is placed in an electrical potential gradient. The transport of the particle through the nanopore is sensed by ion current measurements[78]. Although it is necessary to fundamentally understand the mass transport at the nanoscale, such a single pore membrane with a large diameter would have limited applications in small

molecules or in large-scale separations. It is essential to develop strategies for synthesizing membrane platforms with smaller diameter CNTs for chemical engineering or drug delivery applications.

An important challenge therefore remained: to fabricate and characterize CNT membranes with a large array of CNTs for fundamental mass transport studies, validating some of the MD predictions and developing large area platform applications. Readers interested in fluid transport through CNTs are referred to an outstanding review article by Whitby et al[79].

2.2 Ionic Solution in CNTs

Different aqueous ionic solutions contribute in numerous biological procedures. Based on different applications, aqueous ionic solution systems can be allocated to different classifications: ion transport systems (ion transport in CNTs is desired), ion selectivity systems (ion transport in CNTs is selectively favorable) and ion exclusion systems (ion transport is unfavorable in CNT). One of the main applications of ion exclusion is in water purification. There are also chemical, medical, and industrial applications. The main recent interests in water desalination are based on creating economical methods of producing water in which most of the dissolved salts are ionic. Although technologies like reverse osmosis[80], electrodialysis and membrane distillation for desalination are broadly used, the fabrication of an efficient membrane materials that can isolate salt from water attracts interest as it has the potential of extending fresh water accessibility by making water desalination more economical. The unique water transport property in CNT mentioned in the previous part and

pore sizes comparable with the ions sizes are specifying CNTs as a very favorable option for the exclusion of harmful chemicals, and contaminants from polluted water. Molecular dynamics simulations[81] predicted that CNT membranes with below nanometer pore sizes can offer considerably higher efficiency when applied in a reverse osmosis desalination process. Simulation studies demonstrate, CNTs with (5,5) and (6,6) chiralities can reject 100% of salt, a 680 to 1100 times enhancement over conventional membranes used for reverse osmosis. The success was related to the energy barriers at the openings of these nanotubes, which can govern the transport of ions into the CNT pores. The transport mechanism is linked to the amount of energy needed for the elimination of the hydration layer. In case of water transport through a CNT pore, the residual hydrogen bonds of water molecules inside the CNTs decrease the energy for the entrance.

Ion bio-channels can control many tasks in our body, for instance the electrical impulses transfer to nerves and hormone release. Ion diffusion through the biological channels is assumed to be a simple physical procedure. The properties of ionic diffusion through the CNTs are increasingly being applied as theoretical and experimental replicas for the transmembrane protein channel studies for ion transport across cell membranes. These studies are helping our understanding of how ions permeate through cells. This knowledge will finally guide us to solutions for many human diseases initiated by ion channel malfunction. Selectivity of K^+ from Na^+ ions can be because the removal of K^+ ions from their hydration shells is thermodynamically more desirable than removing the hydration shells from Na^+. This theory can be hypothetically used for both experimental and MD

studies. Furthermore, use of Donnan membrane idea to the transportation of ions under CNT nanoconfinement could contribute to the design and manufacture of novel devices for efficient separation, production of smart materials, and further novel applications[82,83]. These techniques require neither electricity nor pressure gradient for continuous function. These techniques have the potential to recover high purity aluminum in a one-phase process and reuse it in the same plant. Moreover, the CNT devices designed for ion transport and have prospective applications in energy generation, nanosensors, chemical nanoreactors, and ionic field effect transistors[84,85], because the high surface-area-to-volume ratio in CNTs leads to ion separation by a ionic transport method governed by surface charges. The following section focuses on introducing MD simulation work on ionic transport through CNTs, including the fundamental theoretical models employed in MD simulations in order to explain the behavior of ions through nanochannels.

2.3 Molecular Dynamics simulation theories

Currently, molecular dynamics is broadly applied in analysis of kinetics and behavior of biological molecules. Although MD simulation at the nanoscale is limited, MD in modeling of liquids and gases under CNT nanoconfinement is promising and has inspired scientists to apply MD in the study of the performance of ionic solutions inside CNT. Basically, MD relates Newtonian second law and potential energy.

$$m_i \frac{\partial^2 \vec{r}_i}{\partial t^2} = -\frac{\partial}{\partial \vec{r}_i} U_T(\vec{r}_1, \vec{r}_2, ..., \vec{r}_N), \quad i = 1,2,...,N, \tag{2.1}$$

in equation 2.1, m_i is the mass of a atom or molecule i, r_i is its position, and U_T is the potential energy that is related to article positions. The selection of the potential is important as it can determine interactions between the particles in the simulation. To describe electrostatic interactions such as van der Waals attraction and Pauli repulsion, Lennard-Jones potential, is commonly used. The effect of the electrostatic charges of particles to the potential follows Coulomb's law[86].

$$u(r_{ij}) = 4\varepsilon_{ij}\left[\left(\frac{\sigma_{ij}}{r_{ij}}\right)^{12} - \left(\frac{\sigma_{ij}}{r_{ij}}\right)^{6}\right] + \frac{q_i q_j}{r_{ij}} \qquad (2.2)$$

Equation (2.2) indicates a typical interaction potential including the electrostatic charge effect, in which r_{ij} is the distance between particles i and j, q_i is the partial charge allocated to the particle i, and ε_{ij} and σ_{ij} are, respectively, the energy and size parameters achieved by the Lorentz-Berthelot linking rule: potential disappears at the interparticle distance of $\sigma_{ij} = (\sigma_i + \sigma_j)/2$ and has a minimum well depth of $\varepsilon_{ij} = (\varepsilon_i \varepsilon_j)^{1/2}$. Poisson equation (equation 2.3) and Nernst-Planck equation (equation 2.4) are applied for mathematical explanation of the potentials[84,87,88].

$$\nabla^2 \phi(r) = -\frac{1}{\varepsilon \varepsilon_0} \sum_i Z_i \, e n_i \qquad (2.3)$$

$$J_i = -D_i \left(\nabla n_i + \frac{Z_i e n_i}{K_B T}\right) \nabla \phi \qquad (2.4)$$

Considering the equations (2.3) and (2.4), ε is dielectric constant of the solution, ε_0 is the permittivity of vacuum, n_i is the density of ions of ion type i, $Z_i e$ is their charge, J_i is ion flux, and D_i is the diffusivity of ion type i. Equations (2.3) and (2.4) can be

used to determine ionic current in a nanochannel and density of surface charges. When the tube surface charge is in such a condition that the Debye length increases near to the pore radius, repulsion of co-ions conveys selectivity of ions to the nanopore. Therefore, by changing the surface charge, the ion transport can be adjusted. Study of ion hydration in the bulk water compared with CNT nanoconfinement situation is of great importance. MD can be used to define the probability of the ion position P(z,r) out of the distribution function. A free energy profile, G(z), e.g. potential of mean force for the CNT in a one-dimensional situation, can be estimated as shown below:

$$G(z) = -k_B T \, ln \int_0^R P(z,r) dr \qquad (2.5)$$

where T is the temperature, R is the nanotube radius, and k_B is the Boltzmann's constant. Several ab initio MD simulations consider the polarizability of nanotube in the context of density functional theory[89–91]. Depending on delocalized π-electrons the polarizability of the nanotubes varies. For instance, polarizability of metallic CNTs makes ion permeation less desirable than the semiconducting CNTs. Additionally, large computational cost avoids a broad use of ab initio analysis in large structures. Aluru and Xu[91] indicated that when water molecules and ions transport the nanotubes, the metallic SWNT has greater screening effects than the semiconducting SWNTs. These studies suggest that it should be feasible to distinguish between ions with different charges and to distinguish between metallic and semiconducting nanotubes. Leung et al.[90] performed AIMD to show that binding energies for metallic (6,6) SWNT are 2.9 and 1.8 eV for Na^+ and Cl^-, respectively, whereas a much larger (18,18) SWNT demonstrates lower binding energies of 2.2 and 1.1 eV. This finding indicates

that the proposed use of VA-CNT in ion rejection membranes may need thorough reassessment. The authors also mentioned that confined environments and molecular structures could play a major role in the transport and selectivity procedures. Ions act in a similar way in CNTs with diameters larger than 0.96 nm, regardless of the water configuration under nanoconfinement[81,86,88,92,93]. The behavior of ions in CNTs with bigger diameter matches the experimental results[82,94–96].

When liquids are confined in nanoscale, some exceptional properties are evident that are not distinct at macroscales. When the tube size become comparable to the size of the transporting molecules, the interaction between the transported molecules and the CNT surface could act as a leading aspect for the molecule flow procedure, so invalidating the continuum theory and may result in a single case configuration of water[97,98]. These outstanding nanoscale phenomena can be applied not only to transport of water molecules, but also to water as a processing element during the ion transport. The state of the protons in low temperature water in nanotubes is different from other water phases. The temperature of transition between the bulk water and the ice like water phase depends on CNT size and also the interaction between the CNT and water molecules. Understanding of the transporting water phase at room temperature in CNTs with various sizes is of huge interest[99].

We can use MD as a great tool that benefits us to understand CNT transport facts that are challenging or difficult to do by experimental methods. However, all models have their own limitations, and the theories are mainly established for macro scale. Therefore, in using

these models for nanoscale, we need to study the validity of simulation results. The importance of using molecular dynamics is possibly not less than of experimental findings.

2.4 Ion Rejection, Selectivity and Transport

Regarding the behavior of ions in CNTs, it is hard to consider a difference between exclusion, selectivity and transport. For instance, ion transport blockage means ion exclusion, and ion selectivity means rejection of some ion types and transport of some other kinds. Various simulations and experimental studies have revealed some possibilities for favorable processes. Understanding of the relation between driving force and chemical modification for specific example are fundamental, as each one may result in completely diverse applications.

2.4.1 Ion Exclusion

Water is the most plentiful liquid on earth; however, only 3% is clean and drinkable. Consequently, purification and desalination of seawater and salty water are topics of interest. Fornasiero et al.[82] fabricated CNT membranes (with CNT dimensions of less than 2 nm) and studied the ionic solution transport through the CNTs. Hydroxyl, carbonyl, and carboxylic functional groups are chemically grafted on the nanotube opening in order to introduce negative charges to the CNT opening. Ion transport and also exclusion properties of this system were studies, as a function of, pH, solution concentration, and ion dimension. They proved that hydrophobic; sub-2-nm CNT pores, which were negatively charged on the pore entrance, can reject ions and verify that electrostatic forces is accountable for ion exclusion

in CNT pores. Their results agreed well with the Donnan membrane equilibrium model, which provides additional confirmation verifying the effect of electrostatic interaction[83].

Later, Banerjee et al.[100] confirmed that CNTs could be used for water desalination by introducing different charge distributions on the CNT pore opening. Molecular dynamics simulations indicated that when the diverse charge distributions are used, there is significant ion entry into the nanotubes, and the negative charges on SWNTs cause decrease in the ion diffusion to the nanotubes. These findings increase the attractiveness of the CNT-based devices as a system for water purification.

Goldsmith et al.[101] simulated a model for membranes with nanopores of armchair CNTs of different chiralities such as (8,8), (10,10), (12,12), (14,14), and (16,16) with surface modification. Nonequilibrium MD was used to study the flow of NaCl aqueous solution for both uncharged and charges CNTs. In case of CNTs with no charge, the ion flow rates linearly depend on the applied pressure and increased with pore size. The flow ratio of ion transport was smaller than water transport, which was the confirmation of salt exclusion from the ionic solution. However, for the charged CNT, both water and ion transport rates were lower than the case of uncharged CNT, and the smallest (8,8) and (10,10) systems demonstrated complete ion exclusion. Modification of CNT with surface charges caused a reduction in the total flux of water and improved the amount of salt rejected from the system.

As a distillation system based on membranes, Gethard et al.[102] suggested a mixed matrix composed of a polypropylene membrane embedded with evenly distributed, Polyvinylidene fluoride surrounded MWNTs. The hydrophobic property of MWNT

enhanced removal of the $MgSO_4$ and NaCl salts from the ionic solution. As water transport happen in a vapor phase during the distillation procedure, water did not face any permeation barrier. Thus, the filtered water purity was improved. Tofighy et al.[103] suggested a method of using a sheet net of chemically oxidized CNTs to attract salts in ionic solutions, and was tested successfully. Consequently, the capability of MWNT to adsorb toxic heavy metal from water was experimentally explored by Kandah et al.[104], using oxidized MWNT. These Oxidized CNTs were efficient in adsorbing and removing nickel from water. For instance, having negatively charged chemical groups on CNT pores enhance cation adsorption ability. These oxidized CNT structures have been an excellent commercial membrane to be used in removing nickel from water. The application of CNT as a nanochannel for ion rejection devices is a capable route for ion exclusion from aqueous solutions. One of the greatest approaches in the area of ion exclusion is the control of charges and so the electrostatic interactions at the CNT pore opening, because the necessary ion exclusion could be reached by simple approaches like CNT chemical modification or adjusting the pH of the ionic solution.

2.4.2 Ion Selectivity

Comprehending and explaining ion selectivity are fundamental. Channels behave differently towards K^+ and Na^+ ions and this fact is interesting for reaseachers. Ions in aqueous solutions are more energetic because they are hydrated, which are thermodynamically a more favorable state. When pore dimension is smaller than the size of the hydration shell, the ion requires removing the hydration layer in order to enter to the pore.

This method can be applied for gated ion transport by entrance energy barrier modification[88,105–107].

In Peter and Hummer[88] model for CNT membrane, nonpolar pores with diameters of about 5 Å can thoroughly block Na^+ ions, but they transport the ions in case the pore diameters increase to about 10 Å. Shao et al.[86] studied Na^+ and K^+ selectivity inside CNT pores with diameters of 0.60, 0.73, 1.0, 1.28 and 2.00 nm. The smaller CNTs were more favorable for diffusing hydrated K^+. In contrast, in the larger CNTs the situation is different. This study showed that the ion selectivity is linked to the energy needed in order to incorporate the hydrated ion under CNT nanoconfinement.

In another study Gong et al.[108] also showed that selectivity in a (9,9) SWNT could be enhanced by modification of the CNT inner wall by carbonyl oxygen chemical groups. This simulation indicated a significant selectivity, which was related to the hydration of confined K^+ or Na^+, which could be further modified by various arrangements of the carbonyl functional groups. Dzubiella et al[92] used MD simulation in equilibrium and nonequilibrium states and studied the ionic aqueous solution permeation in a hydrophobic pore and investigated the relation of ion and water transport on pore diameter. They reported that the energy barrier at the CNT entry was lower for the K^+ comparing the Na^+ ions. Moreover, when the tube diameter was smaller than a critical value, water had to be driven by an electric field in order to enter the pore. The energy barrier that avoids ion permeation into CNTs decreased to a few k_BT when the electric field that polarized the channel was increased. Comparable results on ion selectivity in charged surroundings were also reported

by Yang et al[109]. They studied the separation of cations with various sizes in negatively charged (5,5) CNT nanopores using MD simulations. In case of low pore charge density, there was no entrance of ions into the CNTs. However, in case of higher pore charge density the ion partitioning was promoted, and the larger ions entered the CNT earlier than smaller ions. Therefore, they proposed the presence of a free energy barrier that can be modified by changing the pore charge density.

Later, Song et al.[110] confirmed pressure controlled ion selectivity in narrow CNTs. They studied SWNTs with diameters of 3.4-6.1 nm to illustrate that Na^+, K^+ and Cl^- ions experience different energy barriers in entering the CNTs. For instance, in the (5,5) tube, the order of free energy barriers is $\Delta G_{Cl-} > \Delta G_{Na+} > \Delta G_{K+}$, meaning K^+ entrance to the SWNT is the easiest. A main impact on the free energy barrier difference was the required energy related with a hydration shell of the ions. Ions in small pores cannot have a coordination number close to their bulk value. So, in this case selectivity was governed by the ion solvation energy. This description could also fit the selectivity in potassium nanochannels. Simulations and experimental studies have predicted the significance of the hydration shells dimension on ion selectivity. There is a correlation between the ions' behavior under CNT nanoconfinement and some biological procedures in our body. Consequently, such studies could help us for inventing cure for illnesses such as Alzheimer's disease, blindness, heart disorders.

2.4.3 Ion transport

Ionic flow through CNTs attracts significant interest from industry because of its potential use in energy applications, and from academia because of the essential influence of the transport mechanisms. Controlled ion transport carries the possibility of applying CNT for using in drug delivery systems, molecular sensors, nanoreactors, and ionic transistors.

Dzubiella et al.[92] explored cation transport in an aqueous solution under equilibrium and nonequilibrium conditions by applying a basic model of hydrophobic pores. Their simulation studies indicated the discontinuous filling of hydrophobic cylindrical pores by water under equilibrium states, provided that the pore radius exceeded a value of R_c = 5.3 Å. Under this critical radius, water could diffuse the pore by application of a robust electric field. It was also confirmed that hydrophobic pores have a lower entrance energy barrier for K^+ than for Na^+, despite the smaller sodium ion size. Lately, experiments and MD simulation performed by Strano et al.[111] showed a CNT-based nanofluidic device. They applied different ionic solutions, induced the transport by a standard clamp method, and monitored currents for different applied electric fields across two reservoirs, which was linked by nanotubes (up to 45) that were 500 mm in length as illustrated in Fig. 2.1. They noticed pore blocking when cations are driven into CNTs, hindering proton current. The proton conductance through the nanochannel could be because of the attraction of protons and exclusion of anions from a negatively charged CNT opening, which was done by oxygen plasma etching. Although stochastic signals in CNT considered comparable to the biological channels, the transport and entrance mechanisms of hydrated ions for CNT differed from the biochannels, because the

quantity of negative charges on CNT pore opening was insufficient, so ions had to be enforced to diffuse the CNT pore. The simulations expected the presence of an optimum rate of proton penetration into the nanopores that increases the ion transport efficiency. They detected a single molecule ionic resonator. Ions can easily diffuse into the CNTs when there are external forces. Based on the MD simulation of potassium ion transport in CNTs[85] driven by electric field, K^+ ions can penetrate CNTs faster when pushed by an external force than when pushed by thermal variations. This conclusion suggests the application of data storage devices in CNTs.

Other MD simulations, by Beu et al.[93] explored the ionic current dependence on CNT diameter. The simulations indicated that the ions in an aqueous solution inside the nanopores encounter considerable energy barriers and can only transport through CNTs larger than (7,7). The (8,8) CNT permits ion diffusion simply, and there is a low current magnitude of approximately 0.05 nA in different circumstances.

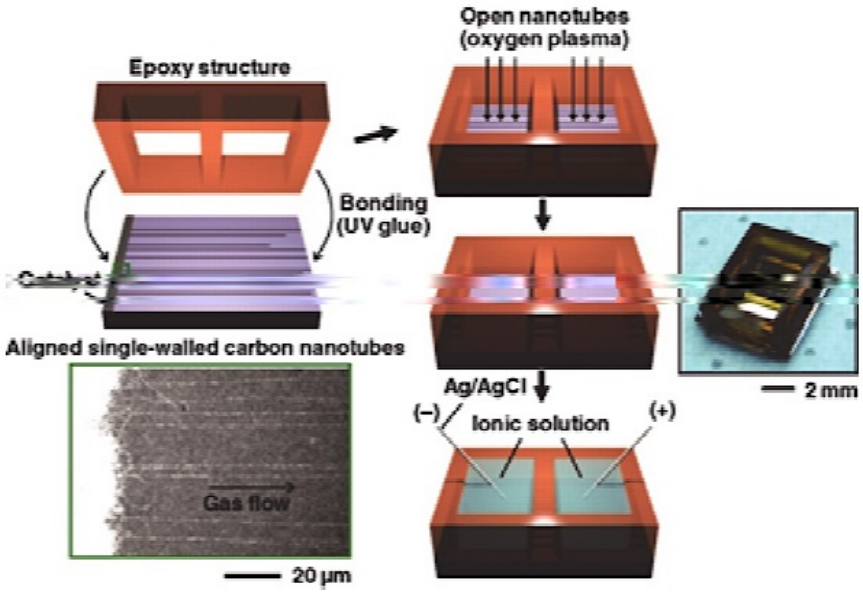

Figure 2-1 : Fabrication of SWNT ion channels. An epoxy structure with two compartments is bonded onto a substrate with ultralong and aligned CVD-grown nanotubes. Reprinted with permission from reference[111]

The ion current or the number of ion transports through CNTs demonstrates a quadratic difference with respect to the CNT pore dimension and disappears when the CNT size becomes around 1.1 nm (for the (8,8) CNT).

There are not much experimental studies of ion transport through CNT compared with MD simulations. Yu et al.[96] experimentally studied ion transport though CNT-based membrane with 3 nm CNT and also 3 nm nanopores. The membrane was made by solvent evaporation method and was used as a perfect model system for exploring ion diffusion through CNTs. Ion transport through CNT membranes blocked after a few hours at the temperature of 298 K, however when the temperature was increased by about 20 K and when

the membrane was exposed to ultrasound sonication, ion transport considerably increased. Water adsorption isotherms for the CNT membranes proposed that the adsorbed water can make a discontinuous phase at the temperature of 293 K, however it can rapidly make a continuous phase at larger temperatures. While the temperature rises or ultrasound sonication opened the tubes, ions diffuse in CNT at a flow rate comparable to the bulk diffusion in aqueous solution. This conclusion implies the application of CNT membranes for water treatment and desalination. Dong et al.[98] did MD simulation of aqueous ionic transport in (9,9) and (10,10) CNTs and they proved evidence of an extraordinary phase behavior of the ionic solution in CNT. Although the amount of cations and anions entered to the CNTs were identical, cations continuously entered faster into the CNTs than anions throughout the whole transport procedure. The hydrogen bonding interaction shows a leading function for cations and anions when enclosed in CNT. Considering the free energy, that can define a driving force of ions and counter ions in entering CNT, clarified that a cation could diffuse in CNT by favorable distribution of Lennard-Jones interactions. However, based on the free energy estimation it is challenging for anions to diffuse the CNT channel instinctively. A more favorable situation would be when an ion permeating a CNT accompanying a cation and it's counter anion by hydrogen bonding.

Water presence is necessary as a process facilitator for transporting ions in CNTs. Ionic current through CNTs is highly related on the CNT size. This evidence suggests one method of controlling ion gating in CNT nanoconfinement. We can also control the ion transport in the nanochannels by regulating electrostatic interactions between ions and the

CNT pores. Merging of the concentration gradient, polarization of CNT, chemical functionalization, and application of an external electric field can make this adjustment to CNT. Most of the times, MD simulations based on simplified water potentials ignore the polarizability effect in simulations. Considering CNT length scale, there is a difference between simulated CNT and CNT used in experiments, the earlier being calculated 1 nm, while the later is in the order of micrometers. Each of the simplifications initiated from considering limits in simulation studies can considerably affect the validity of the data, and so care needs to be taken.

To summarize, molecular dynamics is extensively applied to analyze the behavior of ions inside CNTs, however it is not established enough to study the detailed ionic configuration and ion transport in CNT nanoconfinement. Consequently, there are emerging research opportunities. So far, various interaction potentials have been studied to understand and explain how water and ion behave in nanoscale; but each potential is not valid in capturing the entire picture of the behaviors. Selectivity, exclusion, and transport of ions are all highly linked processes. The relationship between these concepts is based on the same simple mechanisms that control ion behavior in CNTs. In a CNT with small radius, it is the interaction between the water hydration shell of an ion and the opening of the CNT that shows an important role. This interaction can become particularly important to ion exclusion and selectivity. CNTs with larger diameters, transport ions more often than other phenomena. External forces applied to CNT can offer a gated ion transport mechanism. Functionalization of the CNT openings and defect sites can improve an electrostatic interaction between ions

and CNT openings, and can offer another selectivity way to the ion transport. The selectivity mechanism in the ion transport through CNTs can also be influenced by the applying an electric current or by control of pH of the solution. Control of different physical properties related to the ions and CNTs may qualify practical selection among ion selectivity, ion exclusion, and ion transport.

The potential for the use of CNTs for water desalination is motivating researchers to develop new models of simulation and experimental techniques and platforms for studying the exclusion of ions from an aqueous solution. The similarity between CNTs and biological channels is promising to facilitate understanding of the mechanism of selectivity between potassium and sodium ions in the body. Study of ion transport under CNT nanoconfinement propose various applications, such as for nanocontainers for drug delivery systems, nanoreactors, molecular detectors, rectifier circuits and ionic transistors. Eventually, the collaboration between simulation and experimental studies will let to better comprehend the fundamental science concept of ionic behavior under CNT nanoconfinement and to define valuable areas to use in the fundamental science.

2.5 Summary

CNT Nanofluidics studies mass transport phenomena in the nanoscale distinctively occuring inside CNTs. One feature of this transport is the significance of molecular interaction under CNT nanoconfinement between a transporting molecule or ion and carbon wall. While water is confined in CNT, water molecules will face a potential offered by the hexagonal network of carbon atoms. The most important aspects determining water transport

in CNTs is the hydrophobicity, smoothness and curvature of CNTs. Consequently, water transport in large-curvature CNTs will not follow any prediction of continuum theory. CNTs are effective structures for gas transport. A collision process illustrates the transport mechanism for gas. When gas enters a CNT, its momentum relocates from gas to gas collision to gas to CNT collision. In this event, the smoothness of the CNT wall shows a key role by enhancing collisions between gas molecules and the CNT wall, thus improving the transport. Ions inside CNTs can take three paths, i.e., selectivity, exclusion, and transport, based on the dimensional comparison between CNT diameter and the actual hydration shell of the ion. Besides the dimensional relationship, other physical mechanisms can also join in selecting one of the ion transfer paths. These mechanisms include, electric field, electrostatic interaction, and solution pH. Efficient transport of water and gas through CNT can play a role as a main feature for energy efficient filtration, if joined with selectivity mechanisms. Advances in this area could lead to effective water purification, seawater desalination, demineralization, gas separation for greenhouse gas emission improvement, biomolecular separation, DNA sequencing, and more. CNT-based Nanofluidics is rapidly merging fundamental nanoscience and socio-industrial needs, and offers potential for focusing humanity's future sustainability issues.

Chapter 3: Smart DNA Functionalized Carbon Nanotube Membrane Devices

3.1 Introduction

Protein channels are outstanding and fascinating biological systems that can selectively transport essential chemicals through cell membranes faster than inorganic pores can. The fabrication of synthetic membranes with nanopores that mimic biological transmembrane protein channels have numerous applications, ranging from drug delivery, water purification, molecular sieving, to DNA sensing [112–115]. These membranes should possess selective gate chemistry at the pore entrance, a mechanism for fast hydrodynamic flow, and a mechanism to stimulate the channel [116].

There have been several different approaches towards obtaining biomimetic membranes. Previous studies on artificial protein channels have investigated the use of porous alumina or track-etched polycarbonate substrates with well-ordered nanoporous structures and selective chemistry [114,115,117–119]. However, these studies did not offer the capability to create an efficient chemical layer to act as a gatekeeper over the pores. Furthermore, these channels do not offer enhanced hydrodynamic flow.

Recently, carbon nanotubes (CNTs) have been investigated as a biomimetic fluidic channels due to their fast hydrodynamic velocity profiles, highly uniform and tunable pore diameters, and gating capabilities [57,58,72,120–125]. Early molecular dynamics (MD) simulations predicted strong hydrogen bonding of water in hydrophobic CNTs, resulting in a faster hydrodynamic flow rate than that expected for conventional porous platforms[57] and on the

same order as water through Aquaporin-1. MD simulations and experiments have shown that the increased hydrodynamic flow velocities through CNTs can be attributed to the atomic smoothness of the graphitic surface displaying near-perfect slip properties [57,58,72]. In another study, a fast flow rate of molecules was also predicted based on the near frictionless nature of the CNT walls[72,126]. A key challenge in using synthetic membranes is the introduction of reversible gating properties. Gating membranes have been made using stimuli-responsive hydrogels, which exhibit reversible phase changes in response to temperature, pH, or electric charge [127-128]. However, some disadvantages are associated with applying hydrogels [129]. For example, hydrogel membranes have low mechanical stability and low molecular diffusivity [130]. In contrast, CNT membranes, which have been studied in the present report, are remarkable candidates that can be mechanically strong and allow enhanced ion/molecular transport that mimics biological ion channels. Researchers have fabricated MWNT-membranes with specific pore diameters by using vertically aligned MWNT arrays in polymer [131-132] or ceramic matrices. Furthermore, gatekeeper chemistry has been developed for regulating ions and small molecules through CNT membranes; short and long-chain alkanes, negatively charged dye molecules, long polypeptides, and proteins [124,133-134]. In the present work, we design a responsive, smart, controllable CNT membrane by regulating ion transport through an array of vertically aligned carbon nanotubes functionalized with Cy3-T15-NH2 single-stranded DNA embedded in polydimethylsiloxane (PDMS).

The tips of the CNTs with carboxyl end groups were functionalized, forming the basis for gatekeeper-controlled chemical separations or an ion-channel mimetic sensor. If a

selective functional molecule were attached to the entrance of the CNT and coordinated with a bulky receptor, the CNT pore would be blocked and the ionic flow through the CNT core would be reduced[124,133-134]. The ionic flow could be easily detected by electrochemical methods and could offer the basis of a selective sensor device. In the current study, the amino-modified probe DNA (Cy3-T15-NH2) was grafted to the CNT membrane surface followed by cDNA (A15) hybridization.

3.2 Materials and Methods

3.2.1 Synthesis of VA-MWNTs

To make our CNT membrane, the next step was to grow an array of ultra-long, aligned MWNTs (VA-MWNTs) using the CVD-method with high purity ethylene as the carbon source, hydrogen and argon as the carrier gas (70:70:70 sccm) in a 25 mm tube furnace (Lindberg, USA). The growth temperature was 725˚C. Ultra-long, aligned MWNTs were grown for 1 hour. The growth time can be varied depending on the desired length. Figure 3-1 shows the CVD system setup, growth mechanism, and SEM images of as-grown VA-MWNTs.

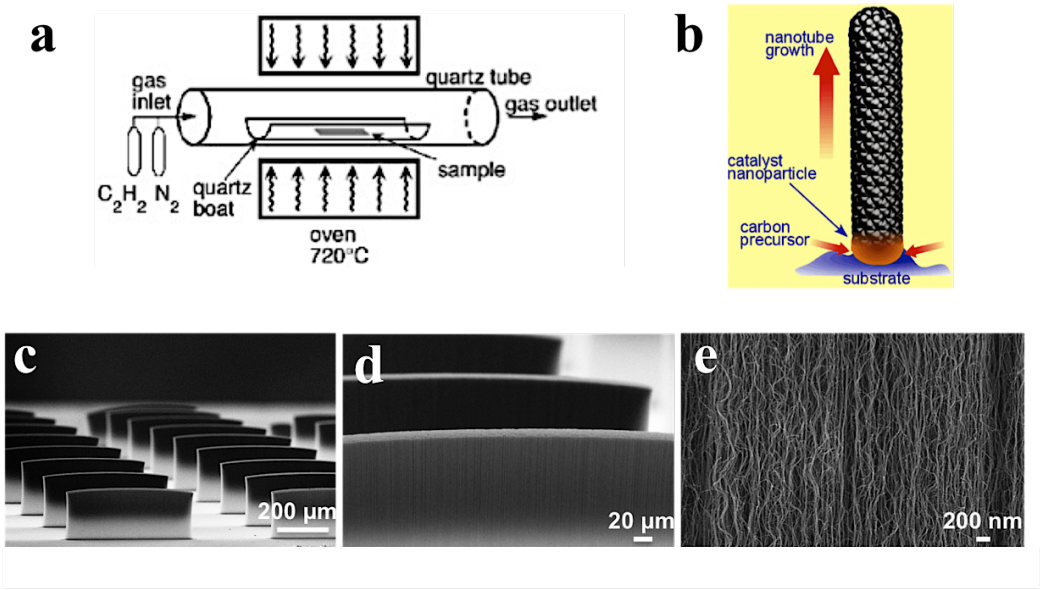

Figure 3-1: Synthesis of vertically aligned MWNTs. (a) Schematic of a CVD system. (b) Illustration of carbon nanotube growth. (c), (d) and (e) SEM images of MWNTs grown by CVD method at 725˚C.

3.2.2 Synthesis of the Membrane and the Control Device

Next, the VA-MWNTs were embedded in polydimethylsiloxane (PDMS, Sylgard 184, 1:10 catalyst: resin ratio) and cured in a vacuum oven for 1 hour at 70°C. The MWNT-PDMS membranes were then submerged in HF for 10 minutes to detach them from the silicon substrate. Following this, the MWNT-PDMS membranes were wet etched in a solution of N-methyl pyrrolidinone (NMP) and tetra-butyl ammonium fluoride (TBAF) for 1.5 hours in order to chemically etch the excess PDMS. The ratio of NMP to TBAF/water was 3:1. TBAF etches PDMS and NMP dissolves the etched material. Subsequently, the membranes were exposed to plasma oxidation for 20 minutes so as to remove excess polymer from the surface and open MWNT tips (Figure 3-5). This process also introduced carboxylic acid functional groups onto the tips of the MWNTs.

3.2.3 DNA Functionalization

Cy3-T15-NH2 single-stranded DNA was grafted onto the tips of the CNTs using carbodiimide chemistry, which has been successful in grafting small and large molecules onto CNT entrances [124,131,135]. The conjugation reaction was carried out overnight at room temperature using carbodiimide chemistry with a final volume of 1 mL containing 10 μM amino-modified probe DNA (Cy3-T15-NH2), 10 mM EDC·HCl (freshly prepared), 25 mM NaCl, and 25mM MES (pH 6.0). After reaction, the solution was removed, and the membrane was washed with 500 μL of deionized water twice to remove free ssDNA. For cDNA hybridization, 200nM cDNA (A15) was added into the 50mM NaCl solution and 50 mM PBS (pH 7.5) with a final volume of 1mL and left overnight. The CNT-ssDNA-cDNA

complex was purified by removing the solution and rinsing the membrane with PBS to remove free cDNA.

3.2.4 Ionic Transport Measurements

The experimental setup consisted of MWNT-PDMS membranes inserted between two additional PDMS O-rings with a 4 mm diameter, which defined the effective membrane area to be 12.56 mm^2. For ion transport experiments, the MWNT-PDMS membranes were clamped between two polystyrene (PS) cuvettes, which functioned as the feed and permeate reservoirs. The experimental setup for measuring ion transport through these DNA-functionalized CNT membranes is shown in Figure 3-2.

At the start of each transport experiment, the feed reservoir, which was previously filled with 1 mL of 0.1 M KCl, was replaced by 1 mL of 1M $[Fe(CN)_6]^{3-}$ .The $[Fe(CN)_6]^{3-}$ solutions were made by dissolving potassium ferricyanide (Sigma-Aldrich) into 0.1 M KCl aqueous solution. The permeate solution were sampled at various time points over 48 hours. In order to prevent any pressure-driven transport, the solution levels were ensured to be the same height on both the feed and permeate sides. The permeate solution was periodically measured using electrochemical measurements using a CHI650A potentiostat (CH Instruments). Differential pulse voltammetry (DPV) was used to determine the potassium ferricyanide concentration. Calibration plots of the potassium ferricyanide solution in the range of 1 to 10^{-7} M were obtained. The detection limit of this technique is 10^{-5} M (Figure 3-3).

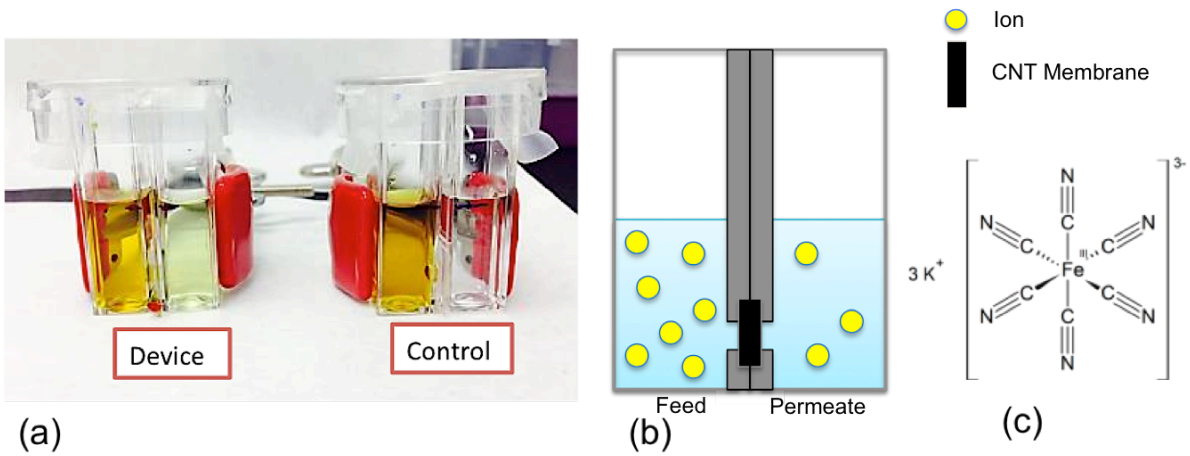

Figure 3-2: Ion transport experimental setup. (a) Picture of two measurement setups. MWNT-PDMS membrane device and PDMS (no MWNT) control membrane are clamped between two couvetts. (b) and (c) Schematic drawings of the experimental setup and the studied $[Fe(CN)_6]^{3-}$ ion.

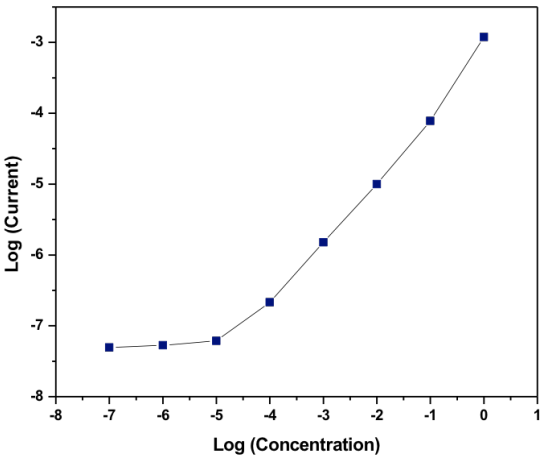

Concentrat	Current(Y)	C(yEr±)
1	0.00119	3.851E-4
0.1	7.809E-5	6.368E-6
0.01	1.002E-5	2.675E-6
1E-3	1.503E-6	3.567E-7
1E-4	2.147E-7	1.589E-8
1E-5	6.11E-8	2.2047E-8
1E-6	5.294E-8	2.0264E-8
1E-7	4.953E-8	1.9686E-8
1E-8	5.716E-8	2.5355E-8
1E-9	7.476E-8	3.6447E-8

Figure 3-3: Calibration curve for DPV detection of potassium ferricynide.

3.2.5 Fluorescence Studies

Fluorescence studies were implemented to qualitatively study the grafting of amino-modified ssDNA (Cy3-T15-NH_2) to the CNT membrane surface. After ssDNA binding, the membrane was washed by deionized water twice and visualized under an inverted epi-fuorescence microscope (Eclipse Ti-S, Nikon) with a CCD camera (Qimaging Retiga 2000R Fast 1394). The excitation wavelength was 540 nm. For comparison, a membrane with no ssDNA binding was also visualized. The fluorescence image of MWNT-PDMS membrane after grafting of ssDNA is shown in figure 3-4. The fluorescence (red) is from the Cy3-labelled ssDNA, confirming the successful conjugation of ssDNA onto the MWNT membrane.

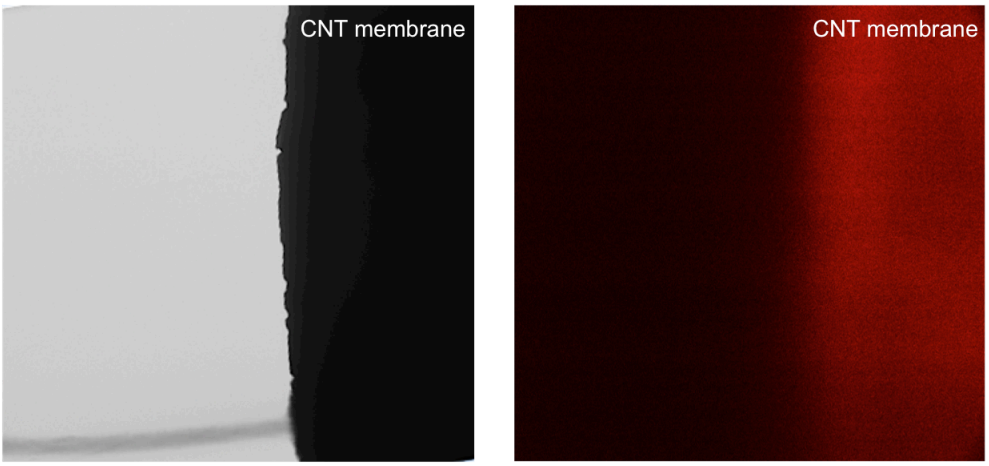

Figure 3-4: Confirmation of ssDNA grafting on MWNT membrane. (a) Transmission white-light image of the membrane before ssDNA grafting. (b) Fluorescence microscopy image of the membrane after ssDNA grafting.

3.3 Results and Discussion

The fabrication procedure for developing CNT membranes is shown in figure 3-5. Vertically aligned CNTs were grown on a silicon substrate using 4 nm Fe as the catalyst and ethylene as the carbon source, as reported[136]. Figure 3-5a includes a scanning electron microscopy (SEM) image of as-grown aligned CNTs, showing the high degree of vertical alignment. Figure 3-5b shows the cleaved edge of the CNT-PDMS membrane. Because of the cleaving process, some of the CNTs are protruding from the surface. The as-grown CNTs had a length of ~ 500 μm, as determined by SEM. To further characterize the as-grown CNTs, they were imaged with a high-resolution transmission electron microscope (HR-

TEM), as shown in Figure 3-6. HR-TEM images confirm that the as-grown CNTs are MWNTs with an inner diameter around 5 nm. During the CVD growth, tube size is defined by the diameter of the iron catalyst particles, which can be seen in the Figure 3-6b inset. Figure 3-6c shows histogram of inner diameters of the MWNTs.

Each MWNT-PDMS membrane contains a large number of MWNTs (~ $4x10^{10}$ tubes/cm^2) (figure 3-5c). This high density allows macroscopic measurement of ion transport through the membrane. Importantly, the open tips of the MWNTs in the membrane were functionalized with carboxylic groups that can be used for further linkage of receptor molecules easily. These receptors can readily bind to a target molecule, which subsequently can open/close the pore entrance. The aim was to switch functionalized nanopore membranes between on and off states reversibly, by attaching and releasing target molecules in a controlled fashion.

In the current study, single-stranded DNA (ssDNA) was anchored to MWNT ends as receptors to enable a reversible on/off system. Specifically, to design a smart membrane, the MWNT pore entrances were functionalized with amine-modified probe ssDNA that binds reversibly to cDNA. The hypothesis is that ion transport through the nanotube pores would be hindered when cDNA binds to the probe ssDNA and restored when cDNA is released. As a result, this study would establish the ability to gate molecular transport through CNT cores for potential applications such as controlled drug release systems and DNA sensing based on molecular gating.

The experimental setup for ion transport measurement through the MWNT-PDMS membrane is shown in figure 3-2. For ion transport measurements, the membrane was clamped between two Polystyrene cuvettes, which acted as the feed and permeate reservoirs. The studied ion is the potassium ferricyanide.

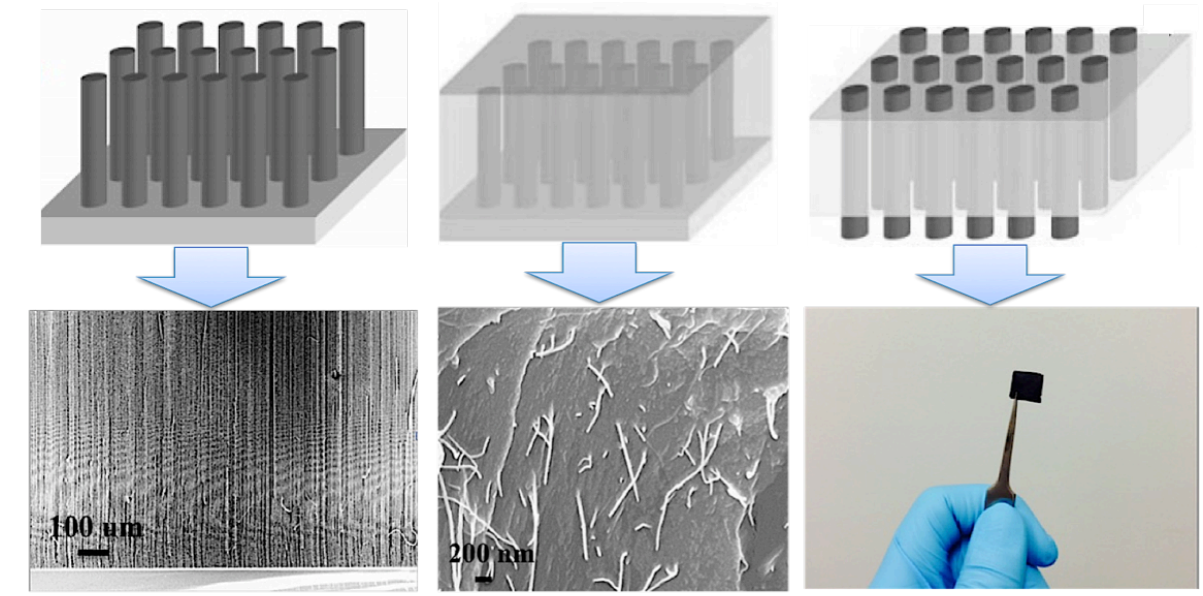

Figure 3-5: Schematic illustration of the experimental steps for the fabrication of membranes with aligned MWNTs (top row), along with the SEM and optical images of the fabricated membrane. Bottom row: (a) SEM of as grown MWNT forest, (b) SEM of a cleaved CNT membrane, and (c) Optical image of the free standing membrane.

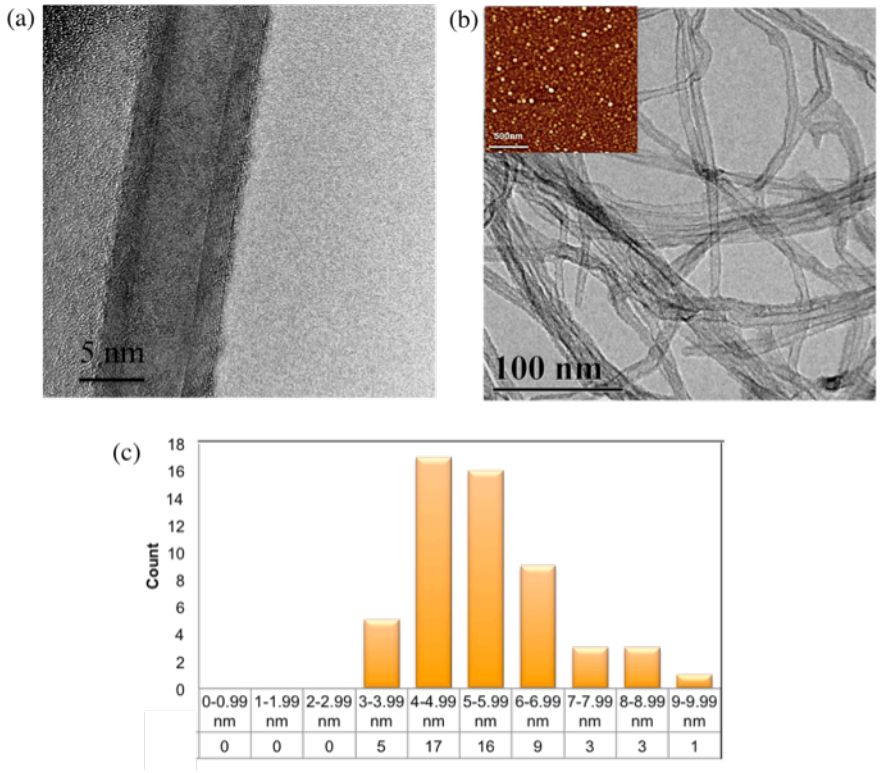

Figure 3-6: TEM characterization of as-grown carbon nanotubes. (a) and (b) HR-TEM images showing MWNTs with 5 nm inner core diameter. Inset: AFM image of the Fe catalyst nanoparticles. (c) Histogram of inner diameters of the MWNTs.

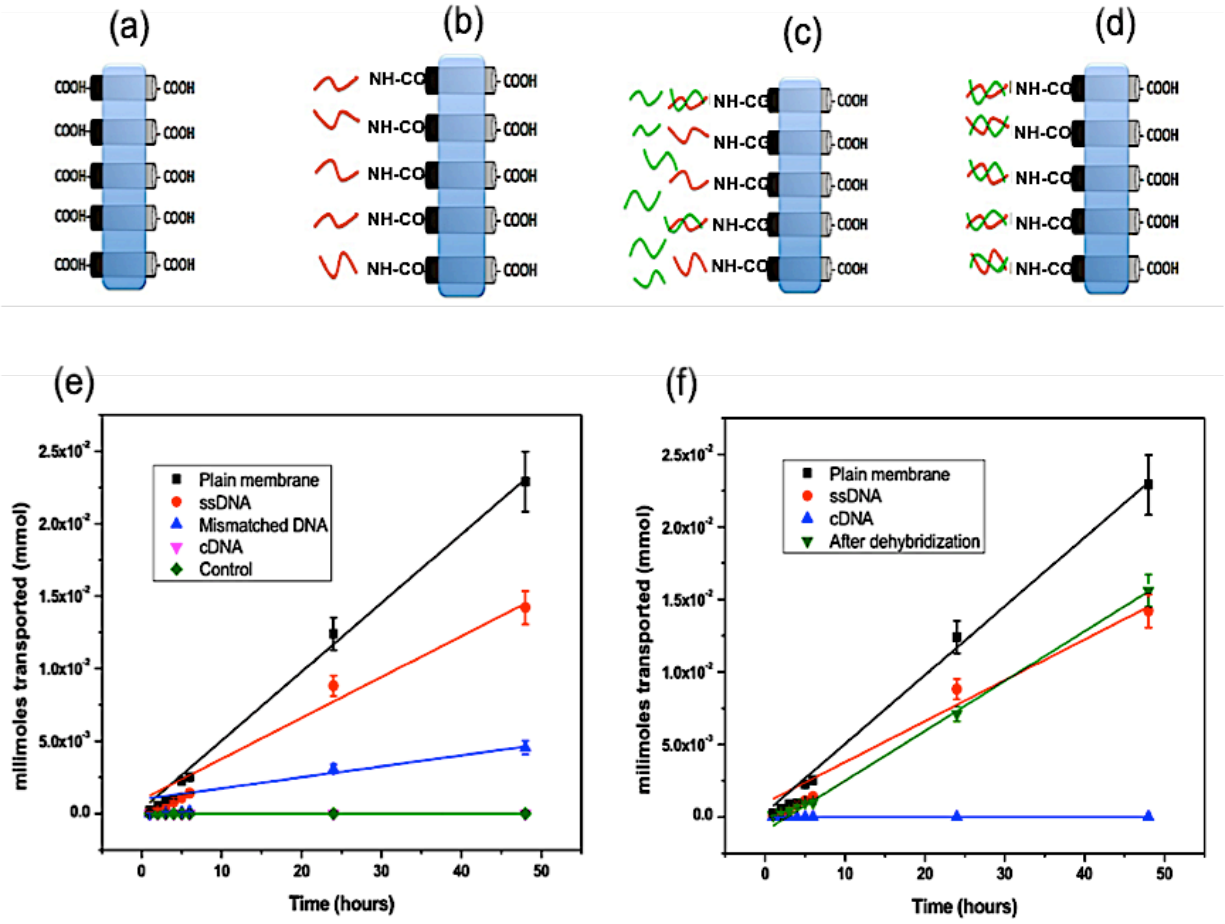

Figure 3-7: Reversible gating of ion transport via DNA hybridization and dehybridization. (a-d) Schematic representation of the CNT membrane as fabricated, after ssDNA functionalization, after exposure to mismatched and complementary DNAs in solution. (e & f) Amount of ferricyanide ions transported through various membranes over time. Control is a PDMS membrane without CNTs.

The diffusive transport of $[Fe(CN)_6]^{3-}$ ions through the CNT membranes was observed, since the ion concentrations in the permeate reservoirs increased progressively over the course of time. The opening and closing of the nanopores was sensed by monitoring the transport of $[Fe(CN)_6]^{3-}$ through the membranes. Using the permeate ion concentrations measured, the moles of ions permeated through the MWNT membranes over 48 hours were calculated and plotted in Figure 3-7e & f. The net flow of ions from the feed to the permeate reservoir was driven exclusively by the concentration gradient across the membrane, which was 1 M originally and assumed to be constant during transport measurements. By applying linear regression to the data points in Figure 3-7e & f, molar flux (*J*) values were taken for each CNT membrane for quantitative comparison.

Table 3-1: Molar Fluxes of $[Fe(CN)_6]^{3-}$ through CNT membranes of different functionalizations

CNT Membrane	*J* (mmol/hr m^2)
Plain	37.7
ssDNA	22.2
Dehybridized	27.3
Mismatched	6.01
cDNA	$< 3.15 \times 10^{-2}$

Before the functionalization of ssDNA to the CNT membranes, a molar flow rate of 4.74×10^{-1} μmol/hr was observed for $[Fe(CN)_6]^{3-}$. We also calculated the theoretical molar flow rate (MFR) through a plain CNT membrane using the following equation,

$$MFR = D\Delta C\left(\frac{A_{eff}}{L_{eff}}\right) \qquad (3-1)$$

where D is the diffusion coefficient of $[Fe(CN)_6]^{3-}$ in water, ΔC is the concentration gradient across the membrane, A_{eff} and L_{eff} are the effective area and thickness of the membrane, respectively. The CNT membranes have an exposed area of 1.256×10^{-1} cm^2, thus A_{eff} is 1.256×10^{-1} $cm^2 \times (\pi r^2) \times N = 2.46 \times 10^{-4}$ cm^2 where r ~ 2.5 nm (the pore radius determined by HR-TEM, as shown in figure 3-6), and N is the number of tubes per unit area (tubes/cm^2). Furthermore, L_{eff} is 5×10^{-2} cm, where L_{eff} is the membrane thickness obtained by SEM. For $[Fe(CN)_6]^{3-}$ permeation through a plain CNT membrane using a 1 M feed, we obtained a molar flow rate of 5.14×10^{-1} μmol/hr or a molar flux of 40.92 mmol/hr m^2. The experimental molar flux obtained is in good agreement with the theoretically calculated value. In the theoretical calculations, we assumed all pores are open by the etching process and are clear of any residual catalyst particles. However, previous studies showed that only 10% of the CNTs are open after plasma treatment[137]. In addition, structural blockages such as bamboo type structures, which are evident in Figure 3-8, further reduce the effective area of the membranes. Even though the exact percentage of CNT lockage is unknown, we suspect that enhanced to ion transport through CNTs is present, in accordance with previous reports [135-138].

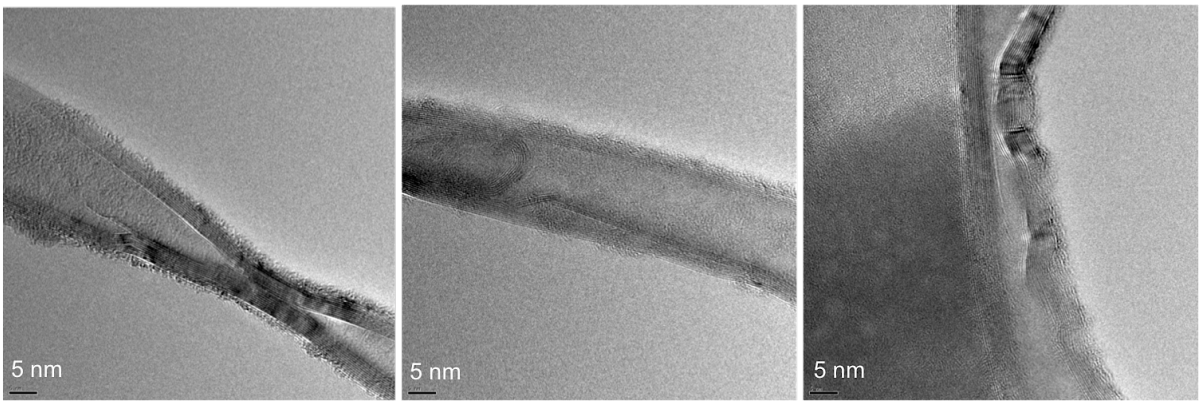

Figure 3-8: HR-TEM images of MWNTs showing structural defects.

A flux of 22.2 mmol/hr m^2 was observed after ssDNA functionalization, suggesting that the attachment of ssDNA to the pore entrances hinders the overall transport of $[Fe(CN)_6]^{3-}$ through the membrane. The presence of chemical moieties at the pore entrance imparts steric and other physical interactions between the solute species and the membrane. In our case, ssDNA binds mismatched or complementary DNA due to nucleobase pairing, altering the pore entrances of the CNT membrane. After incubating the ssDNA-CNT membrane with cDNA, a flux less than 3.15 x 10^{-2} mmol/hr m^2 was measured, indicating ssDNA-cDNA binding lowered the flux of $[Fe(CN)_6]^{3-}$ by three orders of magnitude, sterically blocking the transport of $[Fe(CN_6)]^{3-}$ through the CNT membranes. As the debye length for the studied ionic solution (1 M of $[Fe(CN)_6]^{3-}$ in 0.1 M KCl) is ~ 0.125 nm, the electric double layer does not extend into the pore and the membrane does not exhibit any cationic selectivity and we can conclude that we only have the steric blocking effect in this study.

We also measured the molar flux through the ssDNA-CNT membrane exposed to mismatched DNA (msDNA, AAAAAAACAAAAAAA), which consists of a single-base mismatch at the 8th base position, and the complimentary DNA (cDNA, A15). The binding kinetics of ssDNA-cDNA and ssDNA-msDNA can be predicted using the following equilibrium kinetics equation,

$$K_{eq} = e^{(-\Delta G^0/RT)} \qquad (3\text{-}2)$$

where K_{eq} is the equilibrium constant, R is ideal gas constant (8.314 x 10^{-3} kJ/mol k), T is the temperature (295.15 k) and, ΔG^0 is free energy change due to DNA hybridization. ΔG^0 is equal to 39.215 kJ/mol and 27.408 kJ/mol for cDNA and msDNA respectively. Assuming DNA hybridization on the membrane surface can be described using Langmuir isotherm,

$$K_{eq} = \frac{\theta}{c(1-\theta)} \qquad (3\text{-}3)$$

where c is the initial concentration of DNA, and θ is the equilibrium fraction of hybridized DNAs. In our experiment, c is kept at 10^{-7} M. Considering equation 3-2, the equilibrium constant is equal to 8.76 x 10^6 M^{-1} and 7.1 x 10^4 M^{-1} for both cDNA and msDNA cases respectively. So by considering equation 3-3, the equilibrium fraction of hybridized DNAs is equal to 0.466 and 0.0071 for cDNA and msDNA cases respectively. So the ratio of hybridized cDNA with respect to msDNA case in equilibrium is about 66, which can explain the difference between the molar fluxes for cDNA and msDNA.

Finally, it is worthwhile to note that the dehybridized membrane, which consists of a ssDNA-functionalized CNT membrane after the removal of cDNA, has a molar flux of 27.3

mmol/hr m^2, indicating no loss to ion permeation upon cDNA removal. cDNA hybridization was reversed by heating the membrane for 2 hours in 60°C deionized water, thus restoring the molar flow rate of the ions across the ssDNA modified CNT membrane (Figure 3-7f).

The use of ssDNA-CNT membranes with cDNA regulates the ion permeation through the membrane, displaying reversible on/off characteristics. The use of $[Fe(CN)_6]^{3-}$ as a marker to monitor nucleobase binding offers the means to recognize DNA with single base-pair mismatch.

3.4 Conclusions

In summary, the ion transport across the plain and DNA-functionalized carbon nanotube membranes was studied. The membrane is composed of VA-MWNTs embedded in a PDMS Matrix. The diffusive transport rates of ferricyanide ions were measured in four cases. Therefore, DNA base pairing at the entrance of CNTs is shown to modulate ion permeation through the membrane by steric pore blocking. Furthermore, reversible opening and closing of CNT pores were achieved by the addition and removal of A15 complementary DNA, gating ion transport.

Also, the ssDNA functionalized CNT membrane is capable of recognizing single base-pair mismatches. As a result, this study has demonstrated the ability to gate molecular transport through CNT cores for potential applications such as controlled drug release systems and DNA sensing based on molecular gating achieved with DNAs.

Such ability has led us to design and fabricate novel parallel MWNT nanofluidic devices, which will be discussed in the next chapter.

Chapter 4: Arrayed Multi-walled Carbon Nanotube Nanofluidic Devices

4.1 Introduction

Advances in CNT synthesis methods and experimental design have only recently enabled the make of devices to explore transport through the small diameter CNTs. These devices hold promise as next-generation sensors, platforms for water desalination, ion conduction, energy storage, and to directly probe molecular transport under significant geometric confinement. In this chapter, the development of arrayed MWNT nanofluidic devices is presented. Compared with traditional nanopore devices, these nanotube devices are different. These nanotubes have a remarkably high aspect ratio and so they can confine molecules and also they can increase the translocation time, which possibly result in novel translocation features. The devices have a planar design, which qualifies simultaneous optical and electrical measurements. The devices are designed to have multiple nanofluidic devices on one chip in order to be suitable for simultaneous detection.

4.2 Experimental Methods and Materials

4.2.1 Design and Fabrication of the Arrayed Multi-Walled Carbon Nanotube Nanofluidic Devices

An experimental platform was explicitly designed to characterize ion transport through the interior of CNTs. The devices were fabricated using an epoxy-based material (SU-8), a negative resist that is highly functional and optically transparent. Cured SU-8

(MicroChem) films, or microstructures, are very resistant to solvents, acids, and bases and have excellent thermal and mechanical stability, making them well suited for fabricating permanent structures such as fluidic channels. SU-8 structures acts as an oxygen plasma mask, in order to open the CNT ends, and to form liquid reservoirs at both sides of the CNTs.

The following steps were taken to fabricate the SU-8/PDMS nanofluidic devices.

4.2.1.1 Patterned CVD Growth of Vertically Aligned MWNTs

4.2.1.1.1 Aluminum Oxide Deposition

The first step was aluminum oxide (alumina) deposition. Beginning with a RCA cleaned Si<100>/SiO_2 wafer, 20 nm thick alumina layer was deposited by Atomic Layer Deposition (ALD) technique (Oxford PlasmaLab 100 FlexAL). The alumina acts as a diffusion barrier to reduce the amount of iron that is lost by diffusion into the substrate. It may also mediate the surface mobility of iron as it is heated and thus impact catalyst particle formation.

4.2.1.1.2 Catalyst Photolithography Patterning and Catalyst Deposition

The next step was iron catalyst patterning, which was performed by standard photolithography technique. The patterns were transferred from a photo mask onto the photoresist using UV exposure. Then the exposed areas were washed with a developer and, finally, iron thin film was deposited. The final pattern was rinsed with acetone and isopropanol to remove the photoresist residues. Thus, the iron pattern remained on the substrate where it was directly deposited. If no patterning was done, a thin layer of iron was

deposited on the Si/SiO_2 substrate. The catalyst used was a 4 nm iron (Fe) film, electron beam evaporated on $Si<100>/SiO_2$ wafers. The Fe film was patterned by the standard photolithography technique, using AZ3330 photoresist and LOR5A as the lift-off resist. To obtain maximum process reliability, substrates were cleaned and dried prior to applying the LOR5A resist. The process began with solvent cleaning, rinsing first with dilute acid, followed by DI water. To dehydrate the surface, the wafers were baked at 200°C for 5 minutes on a contact hot plate. An adequate amount of LOR5A was dispensed on the substrate. The dispense spin speed and time were 500 rpm and 5 seconds, respectively. The terminal spin speed was 3000 rpm and the spin time was 45 seconds. The LOR5A coated wafers were baked at 150˚C for 3 minutes and cooled to room temperature. AZ3330 photoresist was then spun onto the substrates. The dispense spin speed and time were 500 rpm and 15 seconds, respectively. The terminal spin speed was 4000 rpm and the spin time was 45 seconds. The AZ3330 coated wafers were baked at 90˚C for 5 minutes. After cooling to room temperature, the samples were patterned by UV exposure machine (Oriel Mask Aligner) at 40 mW/cm^2 for 14 seconds and were post exposure baked at 110˚C for 3 minutes followed by cooling to room temperature. After developing in the AZ300 developer for 45 seconds, the samples were hard baked at 110˚C for 2 minutes. The next fabrication step before growing the MWNTs was electron beam iron deposition, which is shown in Figure 4.1.

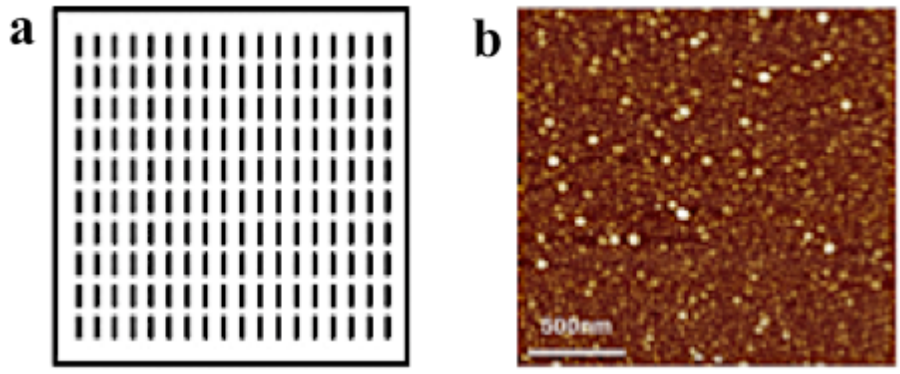

Figure 4-1: Fe catalyst fabrication. (a) Fe catalyst mask design. (b) AFM image of the Fe catalyst nanoparticles, which were annealed at 725˚C.

4.2.1.1.3 CNT Growth by Chemical Vapor Deposition (CVD)

CNT membranes were fabricated as described previously [136]. VA-CNTs with 5 nm pore diameter were grown through chemical vapor deposition (CVD) using high purity ethylene, hydrogen, and argon as the synthesis gases (70:70:70 sccm) in a 1-inch tube furnace (Lindberg). The growth temperature was 725˚C, and the catalyst used was a 4 nm Fe film E-beam evaporated on Si<100>/SiO_2 wafers. The growth time was between 30-60 minutes with no pre-annealing step. The TEM image (Figure 4-2) shows that the CNTs grown by CVD have an average inner diameter of 5 nm, and are well correlated to the density and size of the Fe catalyst particles.

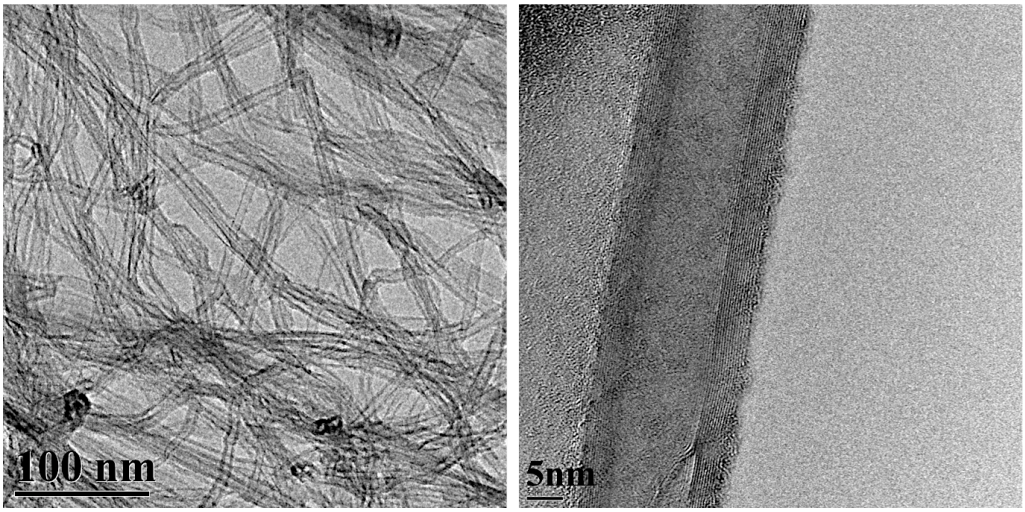

Figure 4-2: TEM images of multi-walled carbon nanotubes grown by CVD method at 725 ˚C using 4 nm Fe thin film

4.2.1.2 VA-MWNT Capillary Folding

Fabricating the nanofluidic devices requires folding of the vertically aligned MWNTs to form horizontally aligned carbon nanotube (HA-CNT) patterns, which is done by a capillary folding method. Figure 4-3 a illustrates the process of capillary folding of VA-CNTs. A thin VA-CNT wall structure was grown by thermal CVD from a lithographically patterned catalyst film. Then a solvent that wets the CNTs (5% ethanol and 95% DI water) was added to a beaker, and the CNT sample was immersed in the solution. As the sample was taken out, it was observed that the wall had collapsed to the substrate, resulting in HA-CNT. The self-directed folding of patterned VA-CNT walls into HA-CNT patches is caused by a mechanical instability induced by capillary forces. The collective deformations and

motions of the CNTs, were caused by both internal and external capillary forces on the CNT forest, as shown in Figure 4-3 a[139]. Figures 4.3 b to e shows the SEM images of the VA-MWNTs before and after folding.

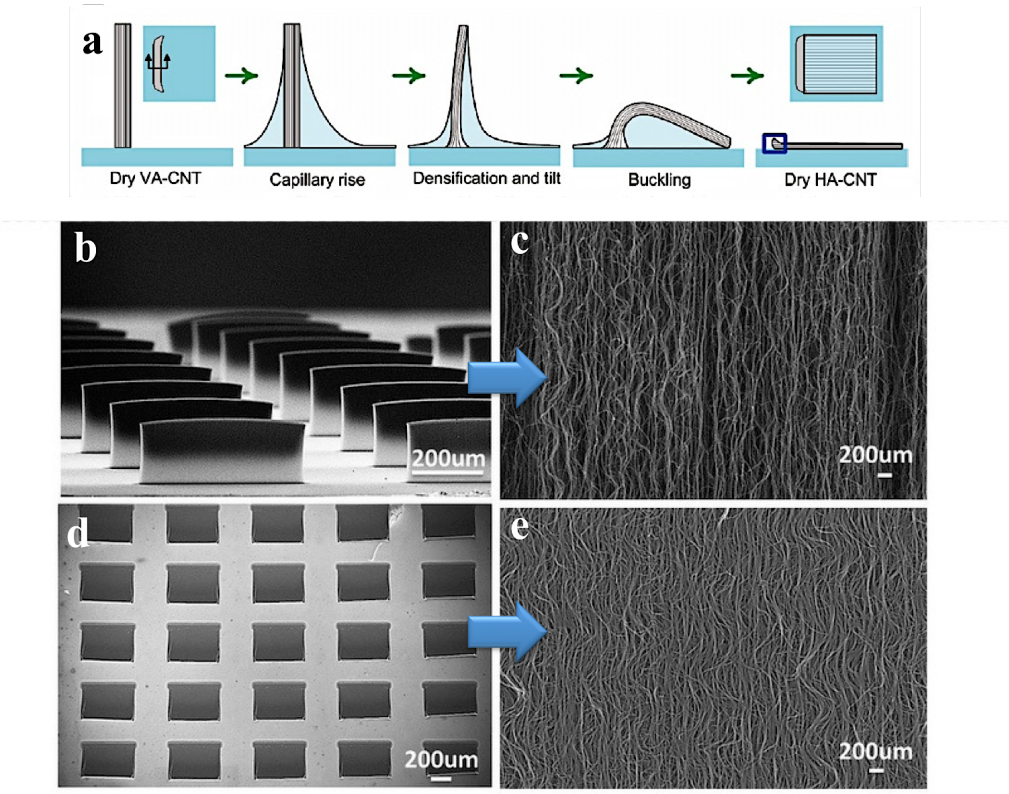

Figure 4-3: Folding of MWNT arrays by capillary folding method (a) step-by-step schematic of structural transformation induced by liquid condensation onto the Silicon substrate (Reprinted with permission from reference 141). (b) and (c) are SEM images of the VA-MWNTs before folding, and (d) and (e) are SEM images of the HA-MWNTs after folding, at different scales.

4.2.1.3 Protecting CNTs and Plasma Etching

Once the HA-MWNT array was made, plasma etching and opening of the CNT ends were carried out. Photolithography was used to fabricate the SU-8 microfluidic structure. This structure not only serves as the microchannel through which to introduce the testing solution, but also is a protective layer to protect the part of the CNTs that should not be etched by oxygen plasma. The SU-8 film was patterned by standard photolithography, using SU-8 2025 (MicroChem) negative photoresist. An adequate amount of SU-8 2025 was dispensed on the HA-MWNT sample. The dispense spin speed and time were 500 rpm and 5 seconds, respectively. The terminal spin speed was 2000 rpm, and the spin time was 30 seconds. The SU-8 coated wafers were baked at 65˚C for 3 minutes and at 95˚C for 6 minutes. After cooling to room temperature, the samples were patterned by UV exposure at 40 mW/cm^2 for 60 seconds (Oriel mask aligner) and were post exposure baked at 65˚C for 1 minute followed by 95˚C for 6 minutes. The samples were then cooled to room temperature and finally developed in SU-8 developer for 3 minutes. Fabrication required an additional step: removing the exposed MWNTs by oxygen plasma etching (Trion Phantom Reactive Ion Etcher (RIE)), and opening both ends at the bottom of the epoxy reservoirs (Figure 4-4). For this step, the RIE condition was as follows: the oxygen flow, chamber pressure and RIE power were 30sccm, 250 mTorr and 100W, respectively. The duration was 5 minutes and was optimized to remove all the exposed MWNTs and to prevent etching of the CNTs underneath the SU-8 layer.

Figure 4-4: Protecting CNTs and oxygen plasma etching (a) SEM image of a HA-MWNT block on the silicon substrate before SU-8 patterning. (b) and (c) Optical images of HA-MWNT block before and after plasma etching.

4.2.1.4 Microfluidic Master Making

To fabricate the microfluidic patterns, soft lithography technique was used. The patterned silicon wafer was plasma etched, producing the silicon master, as follows:

- Depositing 200 nm sputtered Aluminum (Al) deposition, which was used as an RIE mask.
- Al patterning which was prepared by AZ3330 spin coating at 500 rpm for 15 seconds, 400rpm for 45 seconds, 5 minutes soft baking at 90˚C, 14 seconds UV exposing, 3 minutes post exposure baking at 110˚C, 70 seconds developing in AZ300 developer, followed by 2 minutes hard baking at 110˚C.
- Wet etching of Al layer using PAN etch for 1 min at 40˚C.

- RIE of Silicon with the following parameters: 160 mTorr Chamber pressure, 200 W ICP, 20 W RF power, 7 sccm O_2 gas flow, 12 sccm SF_6 gas flow and the etch rate was 0.02 μm/sec)
- Wet etching of Al layer using PAN etch for 1 min at 40˚C.

The next step was PDMS molding and finally bonding the PDMS microfluidic channels to the device, which is described in the next section.

4.2.1.5 PDMS Molding and Bonding

PDMS microfluidic channels were fabricated using standard soft lithography. For this technique, PDMS prepolymer and the curing agent were purchased from Dow Corning (Midland, MI, USA). To begin the fabrication, a photomask design with microchannels was created (CAD/Art Services, Bandon, OR, USA), followed by the previously explained master fabrication process. A plasma etched Si wafer was applied as the master for molding. PDMS prepolymer was thoroughly mixed with its curing agent at a weight ratio of 10:1 and degassed for 30 minutes under vacuum. The mixture was then poured onto the master and cured for 1 h at 80 °C. After curing, the PDMS substrate with a thickness of 2 mm was peeled off from the master, and two, 1 mm diameter holes were punched at the reservoir locations (Figure 4-5).

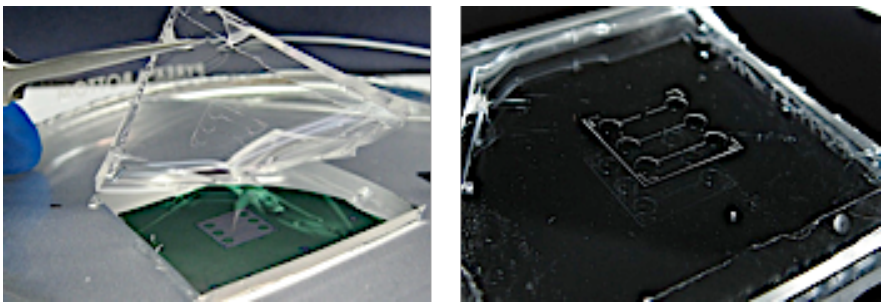

Figure 4-5: Silicon microfluidic master and PDMS Molding

By bonding the PDMS microfluidic channels to the Si/CNT/SU-8 substrate, the final layer was prepared. Specifically, an oxygen plasma treatment of both PDMS and SU-8 surfaces was applied for 20 seconds at 29.6 W. Finally, the two substrates were bonded together. As the PDMS/SU-8 bonding was not strong enough, the following approaches were tried in order to improve the bonding between the PDMS and SU-8:

- Using prime coat as adhesive
- Using uncured PDMS as glue
- Coating a thin layer of uncured SU-8 followed by curing
- Modifying the surface with 3-aminopropyltriethoxysilane (APTES)
- Fabricating Si_3N_4 Shadow mask by protecting SU-8 from burning under oxygen plasma

None of these methods were perfect. Consequently, the device was designed in a different way. This bonding issue was solved by fabricating the device with PDMS. The following steps were taken to fabricate the PDMS device (Figure 4-6):

- Transferring the HA-MWNT onto the PDMS slab substrate. The PDMS slab was made by the same procedure mentioned in chapter 3. The uncured PDMS mixture (10:1 weight ratio) was spin coated on the PDMS slab for 2 minutes at 4000 rpm. Then, the CNT sample and the coated PDMS slab were put together and baked for 1 hour at 80˚C. Eventually, the PDMS slab was peeled off and the HA-MWNT were completely transferred.

- Making the microfluidic master: the master was made by SU-8 photolithography as explained in chapter 3.

- Depositing Al: 100 nm Al was sputtered, making the cured PDMS easier to peel.

- Making PDMS microfluidics: PDMS molding, using soft lithography, enabled the transfer of the pattern.

- Glue bonding of PDMS: the uncured PDMS mixture (10:1 weight ratio) was spin coated on the PDMS slab for 2 minutes at 4000 rpm. The CNT sample and the coated PDMS microchannels were next set together and, to ensure adherence, baked for 1 hour at 80˚C.

- Plasma etching of CNT: the RIE was applied for 25 minutes in a chamber with 50 mTorr pressure, 250 W RF power, 13 sccm O_2 gas flow, and 37 sccm CF_4 gas flow.

- Using Plexiglass to hold the device and to enlarge the reservoirs (Figure 4-6).

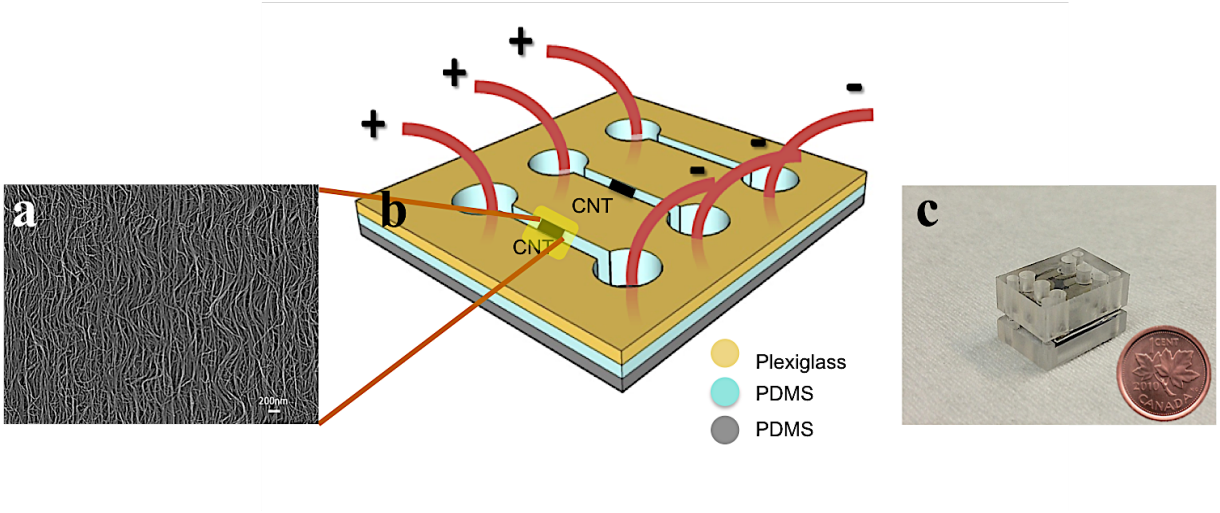

Figure 4-6: Schematics of MWNT ion channel device. (a) Ultra long MWNTs are aligned on a silicon wafer. (b) The PDMS structure covers the MWNTs during the etching process and also acts as a barrier between the two ionic solutions, blocking all molecular transport except that through the MWNTs. (C) Actual picture of the device.

4.3 Results and Discussion

4.3.1 Ionic transport measurement

Once the CNT based nanofluidic device was fabricated, droplets of 1 M sodium chloride (NaCl) in DI water was added to one side of the open-ended nanotubes, i.e. the feed reservoir, and DI water was added to the other side, i.e. the permeate reservoir. The device was then left to air dry over night. Salt crystals were found in the area where the water was initially placed (SEM image, Figure 4-7 C). Elemental analysis by energy dispersive X-ray

spectroscopy (EDX) proved the presence of Na (9.51 atomic %) and Cl (4.33 atomic %) in the permeate reservoir, which have translocated through the CNT-embedded PDMS barrier (Figure 4-7). The same test was performed with potassium ferrocyanide ($C_6N_6FeK_4$), and the EDX results verified the existence of nitrogen (N) (9.75 atomic %), iron (Fe) (1.83 atomic %) and potassium (K) (0.75 atomic %) transported through the CNT-embedded PDMS barrier (Figure 4-8). A transport test through the control devices with no CNTs was also performed and indicated no ion transport through barrier.

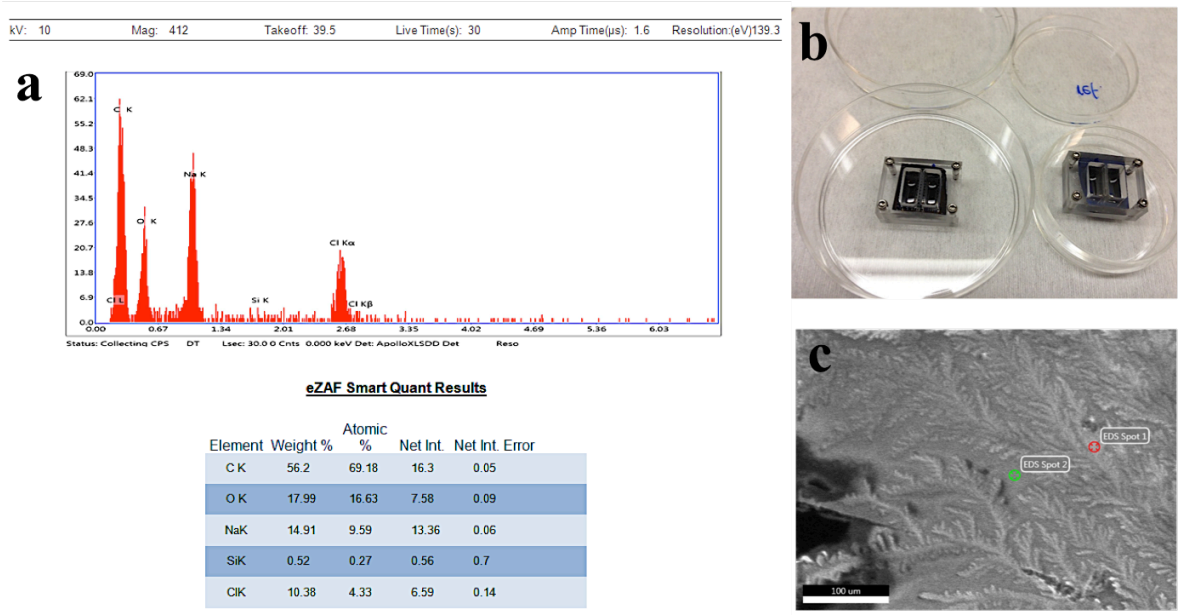

eZAF Smart Quant Results

Element	Weight %	Atomic %	Net Int.	Net Int. Error
C K	56.2	69.18	16.3	0.05
O K	17.99	16.63	7.58	0.09
NaK	14.91	9.59	13.36	0.06
SiK	0.52	0.27	0.56	0.7
ClK	10.38	4.33	6.59	0.14

Figure 4-7: Evidence of ion transport through MWNTs. (a) EDX confirms the NaCl presence in the permeate reservoir. (b) Experimental platform showing droplets of NaCl and water connected by the MWNT arrays. (c) SEM image of NaCl crystals found in the area where the water evaporated.

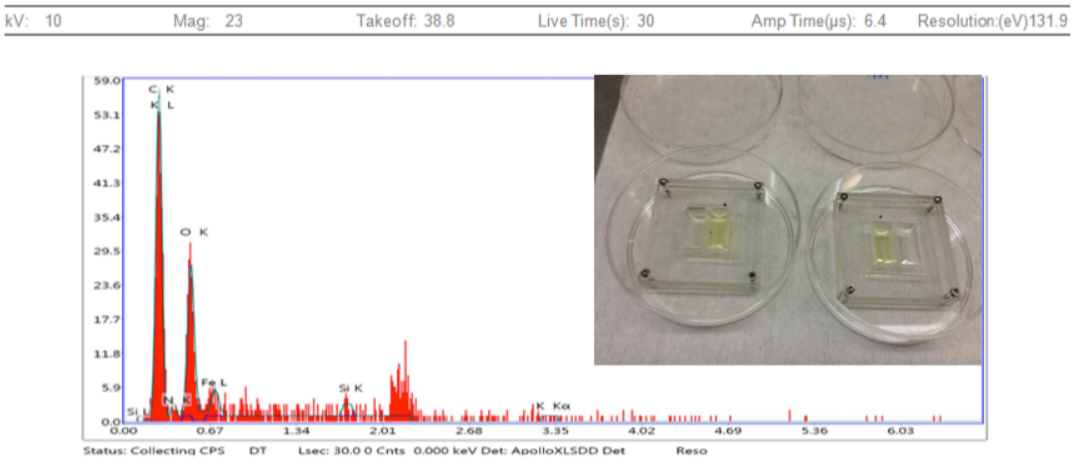

eZAF Smart Quant Results

Element	Weight %	Atomic %	Net Int.	Net Int. Error
C K	49.12	59.08	11.46	0.06
N K	9.45	9.75	0.58	0.62
O K	30.79	27.8	5.79	0.11
Fe L	7.06	1.83	0.65	0.48
Si K	1.54	0.79	0.73	0.7
K K	2.04	0.75	0.39	0.75

Figure 4-8: Evidence of ion transport through MWNTs. EDX confirms the $C_6N_6FeK_4$ presence in the permeate reservoir. Inset: Experimental platform showing droplets of $C_6N_6FeK_4$ and water connected by the MWNT arrays.

4.4 Conclusions and Future Work

In this part of the study, we have designed and fabricated novel CNT nanofluidic devices, by taking use of vertically aligned and ultra-long MWCNTs for the study of the ion

transport and potential applications. Here are some of the important aspects of the project that leads us to the future work.

- There are a lot of simulations and few experimental data (providing experimental conformation to test theoretical models).
- There are long channels to extend the event time and detect the current changes.
- The devices have very high aspect ratio such that they can confine the entire biomolecule.
- The CNTs are long enough to be used for separation applications.
- The CNTs are capable of chemical modification
- The CNTs are capable of doping for ion selective applications.
- Our devices have a planar layout, which could enable simultaneous optical and electrical probing.

We envision many possibilities for new devices with enhanced construction and further analysis methods available, in particular the possibility of DNA sequencing.

Chapter 5: Conclusions and Future Work

5.1 Conclusion

CNTs have been one of the most interesting one-dimensional nanomaterial for years. Many researchers have been studying their outstanding properties in various applications, and have demonstrated that CNTs are attractive materials for making various nanodevices. The exceptionally high aspect ratio, smooth walls, and nanoscale inner diameters of CNTs cause the distinctive phenomenon of ultra-efficient transport of water and gas through these ultra-narrow nanotubes. Water and gas molecules move through nanotube pores orders of magnitude faster than through other pores of comparable size. However, despite the current research, there are still few practical applications of CNTs, due to a lack of understanding about their fundamental properties and potential. CNT membranes are a versatile and truly powerful nanoscale platform for fundamental studies of nanofluidics.

The first part of this Ph.D. thesis has mainly dedicated to the design and fabrication of CNT membrane devices and exploring the ion translocation through a unique CNT membrane device composed of vertically aligned and opened CNTs with inner core diameter of about 5 nm. The main features of the CNT membrane structure are that the pore size is arranged by the inner core of the CNT, making remarkable control over pore size distribution possible; the smooth graphitic inner core lets less interaction between molecules in transition, which leads to high transport ion flow rates; introducing selective chemistry is possible; and the membrane is electrically conductive because of the CNTs crossing. The study sets the foundation for understanding and controlling transport through this novel membrane device.

In summary, DNA-functionalized CNT membranes were designed and used to mimic biological ion channels regulated by nucleobase-pairing of ssDNA. Single-stranded DNA base pairing at the entrance of CNTs is shown to modulate ion permeation through the membrane by steric pore blocking. Furthermore, the fabricated CNT membranes are reversible and are capable of recognizing single base-pair mismatches. As a result, this study has established the membranes' ability to gate molecular transport through CNT cores for potential applications such as controlled drug release systems and DNA sensing based on molecular gating achieved with DNAs.

The major conclusion of the thesis for the first part of the study is as follows:
In chapter 3 mass transports was demonstrated and it exceeds conventional predictions in nanochannels. However, chemical functionalization of the CNT tips introduces enhanced interaction between the solvent and tube opening to reduce the unique flow velocity. Gatekeeper molecular interactions can control the ionic diffusion through a CNT membrane structure.

Taking advantage of carbodiimide chemistry allows the CNT membrane to be covalently attached to functional molecules (ssDNA), changing the gate chemistry, which in turn change the flux and selectivity, as showed in Chapter 3.

A main characteristic of the membrane structure is that it is electronically conductive. The studies done in this thesis are based on concentration gradient ionic diffusion through the CNT membranes. Future research can be focused on studying the effect of potential on the ion transport rate through the CNT membranes.

Learning and considering the results of the ion transport through the CNT membranes discussed in Chapter 3 of the thesis, we moved on to the second part of the thesis (Chapter 4). In it, we report the design and fabrication of devices in which CNT nanofluidic devices, composed of an array of aligned high aspect ratio multiwalled CNTs, span a barrier between two fluid reservoirs. This device is expected to enable direct electrical chronoamperometric measurement of ion transport through the nanotubes and analysis of the ion transport properties. The ion translocation can be probed from ionic current signals.

Our devices have a planar design, which support simultaneous optical and electrical analyzing. The current device structure is compatible with lab-on-a-chip micro-total-analysis systems and microelectronics. CNT nanofluidics is relating fundamental nanoscience and industrial needs, and suggests potential applications for focusing on future sustainability concerns of humankind.

Among myriad applications of transport through the CNT membrane, one of the interesting applications is in using these structures as ionic separations. In this thesis the evidence of steric interactions between permeating molecules and attached molecules on the membranes was demonstrated. A model, consisting of sterically hindered diffusion at the tube entrance and near bulk diffusivity inside the core, could quantitatively describe the fluxes. Also techniques for increasing the attached molecules on the CNT walls to increase the electrostatic/steric interaction are demonstrated. But, a limitation is that the functional molecules on CNT walls will cause the solvent to interact intensely with the walls and will greatly diminish the most attractive feature like high mass transport. So, the best method

would be to have a highly selective chemistry at the CNT end, whereas leaving the inner core of the CNT pristine. More research needs to be done to learn how to increase selectivity without disturbing the permeability through the CNTs. Membranes with large CNT core diameters of about 7 nm appear to be more appropriate for separation of macromolecules. The pore sizes are large and not suitable for gas separation applications, although chemical functionalization could feasibly present some selectivity.

5.2 Directions of Future Work

Future research could be focused on optimization of the functional group density and dimension of the macromolecule in order to improve the efficiency of the device for drug delivery applications. Depending on the application, different functional molecules for different permeates is needed. Additional possible applications would require use of the electrochemical catalytic and fast transport property of the membrane. The CNTs could simply function as catalyst carriers, and the membrane structures could be used as membrane reactors, where mass transport and heterogeneous electrochemical catalysis could be combined to realize Electrochemical Membrane Reactors. Such devices could be promising for fuel cell or environmental applications.

CNT membranes represent an emerging branch of membrane science with numerous opportunities for use in materials science and engineering, and potential applications in different areas related to the environment and energy. Researchers may be inspired by the fact that CNT-based membranes are great choices to advanced materials, like the thin-film composite membranes used for the desalination of seawater. At this point, it may be

worthwhile to restate that this unique class of membranes can provide several competitive advantages, such as very fast liquid and gas transport properties; tighter control over pore-size distribution; chemically modified mass-transport properties; stimuli-responsive behavior; and well-defined nanofluidic frameworks for understanding molecular transport at the nanoscale.

As an example, the array of CNT membranes is potentially attractive for filtration applications such as protein separation. Their electrical conductivity could be useful for flux regeneration and environmental remediation applications such as in electrochemical membrane reactors. Open-ended CNT membranes are being considered for desalination applications, while mixed-matrix membranes could provide materials with novel transport properties for conventional membrane processes, such as membrane distillation or gas separation.

Despite this interest, challenges remain in synthesizing these membranes reproducibly, cost effectively, and with minimum variation of diameters over large areas. For example, desalination membranes for >95% salt rejection would require less than 1 in 100 tubes above 1-nm diameter. These approaches could be controlled at the synthesis stage, that is, with greater understanding and fine-tuning of the growth of nanotubes.

Another approach requires application of diameter-controlled arrangement of CNTs from SWNT suspensions, followed by alignment of CNTs based on self/electric-field-based assembly. To summarize, research on CNT membranes is at a promising stage of evolution. Real-life applications are expected to emerge in the near future. However, several

fundamental and engineering questions still remain unaddressed. Therefore, this highly exciting and remarkable multidisciplinary research area is in need of breakthroughs in nanoscale materials science, composite materials engineering, and better understanding of transport phenomena.

Bibliography

(1) Roco, M. C.; Mirkin, C. a.; Hersam, M. C.; Nanotechnology Research Directions for Societal Needs in 2020: Summary of International Study. Journal of Nanoparticle Research 2011, 13, 897–919.

(2) Iijima, S.; Helical Microtubules of Graphitic Carbon. Nature 1991, 354, 56-58.

(3) Iijima, S.; Single-shell Carbon Nanotubes of 1-nm Diameter. Nature 1993, 363, 603-605.

(4) Dresselhaus, M. S.; Avouris, P. Introduction to Carbon Materials Research. Topics in Applied Physics 2001, 80, 1–9.

(5) Valca, M.; Ca, S. Role of Carbon Nanotubes in Analytical Science. Analytical Chemistry 2007, 79, 4788–4797.

(6) Eder, D. Carbon Nanotube-Inorganic Hybrids. Chemical Reviews 2010, 110, 1348–1385.

(7) Peigney, A.; Laurent, C.; Flahaut, E.; Bacsa, R. R.; Rousset, A. Specific Surface Area of Carbon Nanotubes and Bundles of Carbon Nanotubes. Carbon 2001, 39, 507–514.

(8) Wang, X.; Li, Q.; Xie, J.; Jin, Z.; Wang, J.; Li, Y.; Jiang, K.; Fan, S. Fabrication of Ultralong and Electrically Uniform Single-Walled Carbon Nanotubes on Clean Substrates. Nano Letters 2009, 9, 3137-3141.

(9) Chang, C.; Okawa, D.; Garcia, H.; Majumdar, a.; Zettl, a. Nanotube Phonon Waveguide. Physical Review Letters 2007, 99, 045901.

(10) Ebbesen, T. W.; Electrical Conductivity of Individual Carbon Nanotubes. Nature 1996, 382, 54-56.

(11) Ando, Y.; Zhao, X.; Shimoyama, H.; Sakai, G.; Kaneto, K. Physical Properties of Multiwalled Carbon Nanotubes. International Journal of Inorganic Materials 1999, 1, 77–82.

(12) Yu, C.; Shi, L.; Yao, Z.; Li, D.; Majumdar, A. Thermal Conductance and Thermopower of an Individual Single-Wall Carbon Nanotube. Nano Letters 2005, 9, 1842-1846.

(13) Adu, C. K. W.; Sumanasekera, G. U.; Pradhan, B. K.; Romero, H. E.; Eklund, P. C. Carbon Nanotubes : A Thermoelectric Nano-nose. Chemical Physics Letters 2001, 337, 31–35.

(14) Sumanasekera, G.; Pradhan, B.; Romero, H.; Adu, K.; Eklund, P. Giant Thermopower Effects from Molecular Physisorption on Carbon Nanotubes. Physical Review Letters 2002, 89, 166801.

(15) Cahill, D. G.; Ford, W. K.; Goodson, K. E.; Mahan, G. D.; Majumdar, A.; Maris, H. J.; Merlin, R.; Phillpot, S. R. Nanoscale Thermal Transport. Journal of Applied Physics 2003, 93, 793-818.

(16) Fisher, T. S.; Walker, D. G. Thermal and Electrical Energy Transport and Conversion in Nanoscale Electron Field Emission Processes. Journal of Heat Transfer 2002, 124, 954-962.

(17) Holt, J. K.; Park, H. G.; Wang, Y.; Stadermann, M.; Artyukhin, A. B.; Grigoropoulos, C. P.; Noy, A.; Bakajin, O. Fast Mass Transport Through Sub-2-nanometer Carbon Nanotubes. Science 2006, 312, 1034–1037.

(18) Joselevich, E.; Dai, H.; Liu, J.; Hata, K.; Windle, A. H. Carbon Nanotube Synthesis and Organization. Topics in Applied Physics 2008, 164, 101–164.

(19) Yamada, T.; Namai, T.; Hata, K.; Futaba, D. N.; Mizuno, K.; Fan, J.; Yudasaka, M.; Yumura, M.; Iijima, S. Size-selective Growth of Double-walled Carbon Nanotube Forests from Engineered Iron Catalysts. Nature nanotechnology 2006, 1, 131–136.

(20) Futaba, D.; Hata, K.; Yamada, T.; Mizuno, K.; Yumura, M.; Iijima, S. Kinetics of Water-Assisted Single-Walled Carbon Nanotube Synthesis Revealed by a Time-Evolution Analysis. Physical Review Letters 2005, 95, 056104.

(21) Yun, Y.; Shanov, V.; Tu, Y.; Subramaniam, S.; Schulz, M. J. Growth Mechanism of Long Aligned Multiwall Carbon Nanotube Arrays by Water-assisted Chemical Vapor Deposition. The journal of physical chemistry. B 2006, 110, 23920–23925.

(22) Belin, T.; Epron, F. Characterization Methods of Carbon Nanotubes: a Review. Materials Science and Engineering: B 2005, 119, 105–118.

(23) Avouris, P.; Chen, Z.; Perebeinos, V. Carbon-based Electronics. Nature nanotechnology 2007, 2, 605–615.

(24) Schnorr, J. M.; Swager, T. M. Emerging Applications of Carbon Nanotubes. Chemistry of Materials 2011, 23, 646–657.

(25) Chu, H.; Wei, L.; Cui, R.; Wang, J.; Li, Y. Carbon Nanotubes Combined with Inorganic Nanomaterials: Preparations and Applications. Coordination Chemistry Reviews 2010, 254, 1117–1134.

(26) Vm, S.; Mohamed, A. R.; Abdullah, A. Z.; Chai, S. Role of Reaction and Factors of Carbon Nanotubes Growth in Chemical Vapour Decomposition Process Using Methane — A Highlight. Journal of Nanomaterials 2010, 2010, 1-11.

(27) Brukh, R.; Mitra, S. Mechanism of Carbon Nanotube Growth by CVD. Chemical Physics Letters 2006, 424, 126–132.

(28) Walt A. de Heer.; Aligned Carbon Nanotube Films: Production and Optical and Electronic Properties. Science 1995, 268, 845–857.

(29) Li, W. Z.; Nanotubes Large-Scale Synthesis of Aligned Carbon Nanotubes. Science 1996, 274, 1701–1703.

(30) Ren, Z. F.; Synthesis of Large Arrays of Well-Aligned Carbon Nanotubes on Glass. Science 1998, 282, 1105–1107.

(31) Govindaraj, A.; Carbon Nanotubes by the Metallocene Route. Chemical Physics Letter 1997, 267, 276-280 .

(32) Andrews, R.; Jacques, D.; Rao, A. M.; Derbyshire, F.; Continuous Production of Aligned Carbon Nanotubes : a Step Closer to Commercial Realization. Chemical Physics Letters 1999, 303, 467–474.

(33) Sinnott, S. B.; Andrews, R.; Model of Carbon Nanotube Growth Through Chemical Vapor Deposition. Chemical Physics Letters 1999, 315, 25–30.

(34) Jin, L.; Bower, C.; Zhou, O.; Alignment of Carbon Nanotubes in a Polymer Matrix by Mechanical Stretching. Applied Physics Letters 1998, 73, 1197-1199.

(35) Thostenson, E. T.; Chou, T.; Aligned Multi-walled Carbon Nanotube-reinforced Composites : Processing and Mechanical Characterization. Journal of Physics D: Applied Physics 2002, 35, 77-80.

(36) Smith, B. W.; Benes, Z.; Luzzi, D. E.; Fischer, J. E.; Walters, D. a.; Casavant, M. J.; Schmidt, J.; Smalley, R. E. Structural Anisotropy of Magnetically Aligned Single Wall Carbon Nanotube Films. Applied Physics Letters 2000, 77, 663-665.

(37) Casavant, M. J.; Walters, D. a.; Schmidt, J. J.; Smalley, R. E.; Neat Macroscopic Membranes of Aligned Carbon Nanotubes. Journal of Applied Physics 2003, 93, 2153-2156.

(38) Hata, K.; Futaba, D. N.; Mizuno, K.; Namai, T.; Yumura, M.; Iijima, S.; Water-assisted Highly Efficient Synthesis of Impurity-free Single-walled Carbon Nanotubes. Science 2004, 306, 1362–1364.

(39) Wei, Y. Y.; Eres, G.; Merkulov, V. I.; Lowndes, D. H.; Effect of Catalyst Film Thickness on Carbon Nanotube Growth by Selective Area Chemical Vapor Deposition. Applied Physics Letters 2001, 78, 1394-1396.

(40) Amama, P. B.; Pint, C. L.; Kim, S. M.; McJilton, L.; Eyink, K. G.; Stach, E. a; Hauge, R. H.; Maruyama, B.; Influence of Alumina Type on the Evolution and Activity of Alumina-supported Fe Catalysts in Single-walled Carbon Nanotube Carpet Growth. ACS nano 2010, 4, 895–904.

(41) Zhang, C.; Pisana, S.; Wirth, C. T.; Parvez, a.; Ducati, C.; Hofmann, S.; Robertson, J.; Growth of Aligned Millimeter-long Carbon Nanotube by Chemical Vapor Deposition. Diamond and Related Materials 2008, 17, 1447–1451.

(42) Hinds, B. J.; Chopra, N.; Rantell, T.; Andrews, R.; Gavalas, V.; Bachas, L. G.; Aligned Multiwalled Carbon Nanotube Membranes. Science 2004, 303, 62–65.

(43) Holt, J. K.; Noy, A.; Huser, T.; Eaglesham, D.; Fabrication of a Carbon Nanotube-Embedded Silicon Nitride Membrane for Studies of Nanometer-Scale Mass Transport. Nano Letters 2004, 4, 2245-2250.

(44) Ajayan, P. M.; Tour, J. M.; Q & A Nanotube Composites. Nature 2007, 447, 1066–1068.

(45) Shaffer, B. M. S. P.; Windle, A. H.; Fabrication and Characterization of Carbon Nanotube / Poly (Vinyl Alcohol) Composites. Advanced Materials 1999, 11, 937–941.

(46) Qian, D.; Dickey, E. C.; Andrews, R.; Rantell, T.; Load Transfer and Deformation Mechanisms in Carbon Nanotube-polystyrene Composites. Applied Physics Letters 2000, 76, 2868-2870.

(47) Jung, Y. J.; Kar, S.; Talapatra, S.; Soldano, C.; Viswanathan, G.; Li, X.; Yao, Z.; Ou, F. S.; Aligned Carbon Nanotube − Polymer Hybrid Architectures for Diverse Flexible Electronic Applications. Nano Letters 2006, 6, 413-418.

(48) Raravikar, N. R.; Schadler, L. S.; Vijayaraghavan, A.; Zhao, Y.; Wei, B.; Ajayan, P. M.; Synthesis and Characterization of Thickness-Aligned Carbon Nanotube-Polymer Composite Films. Chemistry of Materials 2005, 3, 974–983.

(49) Safadi, B.; Andrews, R.; Grulke, E. a.; Multiwalled Carbon Nanotube Polymer Composites: Synthesis and Characterization of Thin Films. Journal of Applied Polymer Science 2002, 84, 2660–2669.

(50) Huang, S.; Dai, L.; Plasma Etching for Purification and Controlled Opening of Aligned Carbon Nanotubes. The Journal of Physical Chemistry B 2002, 106, 3543–3545.

(51) Chiang, I. W.; Brinson, B. E.; Smalley, R. E.; Margrave, J. L.; Hauge, R. H.; Purification and Characterization of Single-Wall Carbon Nanotubes. Journal of Physicsl Chemistry B 2001, 105, 157–1161.

(52) Chopra, N.; Selective Growth of Carbon Nanotubes and Oxide Nanowires: Applications in Shadow Lithography and Fabrication of Aligned Carbon Nanotube Membranes, University of Kentucky Doctoral Thesis 2006.

(53) Naguib, N.; Ye, H.; Gogotsi, Y.; Yazicioglu, A. G.; Megaridis, C. M.; Yoshimura, M.; Observation of Water Confined in Nanometer Channels of Closed Carbon Nanotubes. Nano Letters 2004, 4, 2237-2243.

(54) Kolesnikov, a. I.; Loong, C.-K.; De Souza, N. R.; Burnham, C. J.; Moravsky, a. P.; Anomalously Soft Dynamics of Water in Carbon Nanotubes. Physica B: Condensed Matter 2006, 385-386, 272–274.

(55) Agre, P.; King, L. S.; Yasui, M.; Guggino, W. B.; Ottersen, O. P.; Fujiyoshi, Y.; Engel, a.; Nielsen, S.; Aquaporin Water Channels - from Atomic Structure to Clinical Medicine. The Journal of Physiology 2002, 542, 3–16.

(56) Agre, P. Aquaporin Water Channels (Nobel Lecture). Angewandte Chemie 2004, 43, 4278–4290.

(57) Hummer, G.; Rasaiah, J. C.; Noworyta, J. P.; Water Conduction Through the Hydrophobic Channel of a Carbon Nanotube. Nature 2001, 414, 188–190.

(58) Kalra, A.; Garde, S.; Hummer, G. Osmotic Water Transport Through Carbon Nanotube Membranes. Proceedings of the National Academy of Sciences of the United States of America 2003, 100, 10175–10180.

(59) Skoulidas, A.; Ackerman, D.; Johnson, J.; Sholl, D.; Rapid Transport of Gases in Carbon Nanotubes. Physical Review Letters 2002, 89, 185901.

(60) Lai, Z.; Bonilla, G.; Diaz, I.; Nery, J. G.; Sujaoti, K.; Amat, M. a; Kokkoli, E.; Terasaki, O.; Thompson, R. W.; Tsapatsis, M. et al.; Microstructural Optimization of a Zeolite Membrane for Organic Vapor Separation. Science 2003, 300, 456–460.

(61) Li, J.; Papadopoulos, C.; Xu, J. M.; Moskovits, M.; Highly-ordered Carbon Nanotube Arrays for Electronics Applications. Applied Physics Letters 1999, 75, 367-369.

(62) Subramaniam, A. B.; Abkarian, M.; Mahadevan, L.; Stone, H. a.; Colloid Science: Non-spherical Bubbles. Nature 2005, 438, 930.

(63) Cui, H.; Zhou, O.; Stoner, B. R.; Deposition of Aligned Bamboo-like Carbon Nanotubes via Microwave Plasma Enhanced Chemical Vapor Deposition. Journal of Applied Physics 2000, 88, 6072-6074.

(64) Maruyama, S.; Einarsson, E.; Murakami, Y.; Edamura, T.; Growth Process of Vertically Aligned Single-walled Carbon Nanotubes. Chemical Physics Letters 2005, 403, 320–323.

(65) Wang, Y. Y.; Gupta, S.; Nemanich, R. J.; Liu, Z. J.; Qin, L. C., Hollow to Bamboolike Internal Structure Transition Observed in Carbon Nanotube Films. Journal of Applied Physics 2005, 98, 014312.

(66) Ajayan, P. M.; Capillarity-induced filling of carbon nanotube. Nature 1993, 361, 333-334.

(67) Ajayan, P. M.; Opening Carbon Nanotubes with Oxygen and Implications for Filling. Nature 1993, 362, 522-525.

(68) Ajayan, P. M.; Carbon Nanotubes as Removable Templates for Metal Oxide Nanocomposites and Nanostructures. Nature 1995, 375, 564-567.

(69) Dujardin, B. E.; Ebbesen, T. W.; Krishnan, A.; Treacy, M. M. J.; Wetting of Single Shell Carbon Nanotubes. Advanced Materials 1998, 08536, 1472–1475.

(70) Mao, Z.; Sinnott, S.; Predictions of a Spiral Diffusion Path for Nonspherical Organic Molecules in Carbon Nanotubes. Physical Review Letters 2002, 89, 278301.

(71) Sokhan, V. P.; Nicholson, D.; Quirke, N.; Fluid Flow in Nanopores: An Examination of Hydrodynamic Boundary Conditions. The Journal of Chemical Physics 2001, 115, 3878-3887.

(72) Sokhan, V. P.; Nicholson, D.; Quirke, N.; Fluid Flow in Nanopores: Accurate Boundary Conditions for Carbon Nanotubes. The Journal of Chemical Physics 2002, 117, 8531-8539.

(73) Supple, S.; Quirke, N.; Rapid Imbibition of Fluids in Carbon Nanotubes. Physical Review Letters 2003, 90, 214501.

(74) Zhu, F.; Schulten, K.; Water and Proton Conduction Through Carbon Nanotubes as Models for Biological Channels. BioPhysical Journal 2003, 85, 236–244.

(75) Ghosh, S.; Sood, a K.; Kumar, N.; Carbon Nanotube Flow Sensors. Science 2003, 299, 1042–1044.

(76) Megaridis, C. M.; Güvenç Yazicioglu, A.; Libera, J. a.; Gogotsi, Y.; Attoliter Fluid Experiments in Individual Closed-end Carbon Nanotubes: Liquid Film and Fluid Interface Dynamics. Physics of Fluids 2002, 14, L5.

(77) Sun, L.; Crooks, R. M.; Single Carbon Nanotube Membranes : A Well-Defined Model for Studying Mass Transport Through Nanoporous Materials. Journal of American Chemical Society 2000, 122, 12340–12345.

(78) Ito, T.; Sun, L.; Crooks, R. M.; Simultaneous Determination of the Size and Surface Charge of Individual Nanoparticles Using a Carbon Nanotube-Based Coulter Counter. Analytical Chemistry 2003, 75, 2399–2406.

(79) Whitby, M.; Quirke, N.; Fluid Flow in Carbon Nanotubes and Nanopipes. Nature nanotechnology 2007, 2, 87–94.

(80) Suk, M. E.; Raghunathan, a. V.; Aluru, N. R.; Fast Reverse Osmosis Using Boron Nitride and Carbon Nanotubes. Applied Physics Letters 2008, 92, 133120.

(81) Corry, B.; Designing Carbon Nanotube Membranes for Efficient Water Desalination. Journal of Physicsl Chemistry B 2008, 112, 1427–1434.

(82) Fornasiero, F.; Park, H. G.; Holt, J. K.; Stadermann, M.; Grigoropoulos, C. P.; Noy, A.; Bakajin, O.; Ion Exclusion by Sub-2-nm Carbon Nanotube Pores. Proceedings of the National Academy of Sciences of the United States of America 2008, 105, 17250–17255.

(83) Sengupta, A. K.; The Donnan Membrane Principle : Opportunities for Sustainable Engineered Processes and Materials. Environmental Science and Technology 2010, 44, 1161–1166.

(84) Daiguji, H.; Yang, P.; Majumdar, A.; Ion Transport in Nanofluidic Channels. Nano Letters 2004, 4, 137-142.

(85) Kang, J. W.; Byun, K. R.; Lee, J. Y.; Kong, S. C.; Choi, Y. W.; Hwang, H. J.; Molecular Dynamics Study on the Field Effect Ion Transport in Carbon Nanotube. Physica E: Low-dimensional Systems and Nanostructures 2004, 24, 349–354.

(86) Shao, Q.; Zhou, J.; Lu, L.; Lu, X.; Zhu, Y.; Jiang, S.; Anomalous Hydration Shell Order of Na + and K + Inside Carbon Nanotubes. Nano letter 2009, 9, 989-994.

(87) Coalson, R. D.; Kurnikova, M. G.; Poisson – Nernst – Planck Theory Approach to the Calculation of Current Through Biological Ion Channels. IEEE Transaction on Nanobioscience 2005, 4, 81–93.

(88) Peter, C.; Hummer, G.; Ion Transport Through Membrane-spanning Nanopores Studied by Molecular Dynamics Simulations and Continuum Electrostatics Calculations. Biophysical journal 2005, 89, 2222–2234.

(89) Eschermann, J. F.; Li, Y.; Van der Straaten, T. a.; Ravaioli, U.; Self-consistent Ion Transport Simulation in Carbon Nanotube Channels. Journal of Computational Electronics 2006, 5, 455–457.

(90) Leung, K.; Marsman, M.; Energies of Ions in Water and Nanopores Within Density Functional Theory Energies of Ions in Water and Nanopores Within Density Functional Theory. The Journal of Chemical Physics 2007, 127, 154722.

(91) Xu, Y.; Aluru, N. R.; Carbon Nanotube Screening Effects on the Water-ion Channels Carbon Nanotube Screening Effects on the Water-ion Channels. Applied Physics Letter 2008, 93, 043122.

(92) Dzubiella, J.; Hansen, J.-P.; Electric-field-controlled Water and Ion Permeation of a Hydrophobic Nanopore. The Journal of chemical physics 2005, 122, 234706.

(93) Beu, T. a.; Molecular Dynamics Simulations of Ion Transport Through Carbon Nanotubes. I. Influence of Geometry, Ion Specificity, and Many-body Interactions. The Journal of chemical physics 2010, 132, 164513.

(94) Strogatz, S. H.; Abrams, D. M.; McRobie, A.; Eckhardt, B.; Ott, E.; Theoretical Mechanics: Crowd Synchrony on the Millennium Bridge. Nature 2005, 438, 43–44.

(95) Lee, C. Y.; Choi, W.; Han, J.-H.; Strano, M. S.; Coherence Resonance in a Single-walled Carbon Nanotube Ion Channel. Science 2010, 329, 1320–1324.

(96) Yu, M.; Funke, H. H.; Falconer, J. L.; Noble, R. D.; Gated Ion Transport Through Dense Carbon Nanotube Membranes. Journal of the American Chemical Society 2010, 132, 8285–8290.

(97) Levinger, N. E. Chemistry: Water in Confinement. Science 2002, 298, 1722–1723.

(98) Dong, K.; Zhou, G.; Liu, X.; Yao, X.; Zhang, S.; Structural Evidence for the Ordered Crystallites of Ionic Liquid in Confined Carbon Nanotubes. The Journal od Physicsl Chemistry C 2009, 113, 10013–10020.

(99) Reiter, G.; Burnham, C.; Homouz, D.; Platzman, P.; Mayers, J.; Abdul-Redah, T.; Moravsky, a.; Li, J.; Loong, C.-K.; Kolesnikov, a.; Anomalous Behavior of Proton Zero Point Motion in Water Confined in Carbon Nanotubes. Physical Review Letters 2006, 97, 247801.

(100) Banerjee, S.; Murad, S.; Puri, I. K.; Preferential Ion and Water Intake Using Charged Carbon Nanotubes. Chemical Physics Letters 2007, 434, 292–296.

(101) Goldsmith, J.; Martens, C. C.; Molecular Dynamics Simulation of Salt Rejection in Model Surface-Modified Nanopores. The Journal of Physical Chemistry Letters 2010, 1, 528–535.

(102) Gethard, K.; Sae-khow, O.; Mitra, S.; Water Desalination Using Carbon-Nanotube-Enhanced Membrane Distillation. ACS Applied Materials and Interfaces 2011, 3, 110–114.

(103) Tofighy, M. A.; Mohammadi, T.; Salty Water Desalination Using Carbon Nanotube Sheets. Desalination 2010, 258, 182–186.

(104) Kandah, M. I.; Meunier, J.-L.; Removal of Nickel Ions from Water by Multi-walled Carbon Nanotubes. Journal of hazardous materials 2007, 146, 283–288.

(105) Beckstein, O.; Tai, K.; Sansom, M. S. P.; Not Ions Alone : Barriers to Ion Permeation in Nanopores and Channels. Journal of American Chemical Society 2004, 126, 4694–14695.

(106) Alexiadis, A.; Kassinos, S.; Molecular Simulation of Water in Carbon Nanotubes. Chemical Reviews 2008, 108, 5014–5034.

(107) Rasaiah, J. C.; Garde, S.; Hummer, G.; Water in Nonpolar Confinement: From Nanotubes to Proteins and Beyond. Annual review of physical chemistry 2008, 59, 713–740.

(108) Gong, X.; Li, J.; Xu, K.; Wang, J.; Yang, H.; A Controllable Molecular Sieve for Na^+ and K^+ Ions. Journal of the American Chemical Society 2010, 132, 1873–1877.

(109) Yang, L.; Garde, S.; Modeling the Selective Partitioning of Cations into Negatively Charged Nanopores in Water. The Journal of chemical physics 2007, 126, 084706.

(110) Song, C.; Corry, B.; Intrinsic Ion Selectivity of Narrow Hydrophobic Pores. The Journal of Physicsl Chemistry B 2009, 113, 7642–7649.

(111) Kim, W.; Lee, C. Y.; Kevin, P. O.; Plombon, J. J.; Blackwell, J. M.; Strano, M. S.; Connecting Single Molecule Electrical Measurements to Ensemble Spectroscopic Properties for Quantification of Single-Walled Carbon Nanotube Separation. Journal of the American Chemical Society 2009, 131, 3128–3129.

(112) Sugawara, M.; Ion Channel Sensors. Analytical Chemistry 1987, 59, 2842-2846.

(113) Antonenko, Y. N.; Rokitskaya, T. I.; Kotova, E. a; Reznik, G. O.; Sano, T.; Cantor, C. R.; Effect of Streptavidins with Varying Biotin Binding Affinities on the Properties of Biotinylated Gramicidin Channels. Biochemistry 2004, 43, 4575–4582.

(114) Steinle, E. D.; Mitchell, D. T.; Wirtz, M.; Lee, S. B.; Young, V. Y.; Martin, C. R.; Ion Channel Mimetic Micropore and Nanotube Membrane Sensors. Analytical chemistry 2002, 74, 2416–2422.

(115) Lee, S. B.; Mitchell, D. T.; Trofin, L.; Nevanen, T. K.; Söderlund, H.; Martin, C. R.; Antibody-based Bio-nanotube Membranes for Enantiomeric Drug Separations. Science 2002, 296, 2198–2200.

(116) Murata, K.; Mitsuoka, K.; Hirai, T.; Walz, T.; Agre, P.; Heymann, J. B.; Engel, a; Fujiyoshi, Y.; Structural Determinants of Water Permeation Through Aquaporin-1. Nature 2000, 407, 599–605.

(117) Jirage, K. B.; Nanotubule-Based Molecular-Filtration Membranes. Science 1997, 278, 655–658.

(118) Martin, B. C. R.; Nishizawa, M.; Jirage, K.; Kang, M.; Lee, S. B.; Controlling Ion-Transport Selectivity in Gold Nanotubule Membranes. Advanced Material 2001, 13, 1351–1362.

(119) Miller, S. a; Young, V. Y.; Martin, C. R.; Electroosmotic Flow in Template-prepared Carbon Nanotube Membranes. Journal of the American Chemical Society 2001, 123, 12335–12342.

(120) Hinds, B. J.; Chopra, N.; Rantell, T.; Andrews, R.; Gavalas, V.; Bachas, L. G.; Aligned Multiwalled Carbon Nanotube Membranes. Science 2004, 303, 62–65.

(121) Holt, J. K.; Park, H. G.; Wang, Y.; Stadermann, M.; Artyukhin, A. B.; Grigoropoulos, C. P.; Noy, A.; Bakajin, O.; Fast Mass Transport Through Sub-2-nanometer Carbon Nanotubes. Science 2006, 312, 1034–1037.

(122) Krishnakumar, P.; Tiwari, P. B.; Staples, S.; Luo, T.; Darici, Y.; He, J.; Lindsay, S. M.; Mass Transport Through Vertically Aligned Large Diameter MWCNTs Embedded in Parylene. Nanotechnology 2012, 23, 455101.

(123) Nednoor, P.; Chopra, N.; Gavalas, V.; Bachas, L. G.; Hinds, B. J.; Reversible Biochemical Switching of Ionic Transport Through Aligned Carbon Nanotube Membranes. Chemistry of Materials 2005, 17, 3595–3599.

(124) Nednoor, P.; Gavalas, V. G.; Chopra, N.; Hinds, B. J.; Bachas, L. G.; Carbon Nanotube Based Biomimetic Membranes: Mimicking Protein Channels Regulated by Phosphorylation. Journal of Materials Chemistry 2007, 17, 1755-1757.

(125) Majumder, M.; Chopra, N.; Hinds, B. J.; Effect of Tip Functionalization on Transport Through Vertically Oriented Carbon Nanotube Membranes. Journal of the American Chemical Society 2005, 127, 9062–9070.

(126) Ohba, T.; Kanoh, H.; Kaneko, K.; Structures and Stability of Water Nanoclusters in Hydrophobic Nanospaces. Nano letters 2005, 5, 227–230.

(127) Sugawara, M.; Kojima, K.; Sazawa, H.; Umezawa, Y.; Ion-channel Sensors. Analytical chemistry 1987, 59, 2842–2846.

(128) Hoffman, A. S.; Stayton, P. S.; Bulmus, V.; Chen, G.; Chen, J.; Cheung, C.; Chilkoti, A.; Ding, Z.; Dong, L.; Fong, R. et al.; Really Smart Bioconjugates of Smart Polymers and Receptor Proteins. Journal of Biomedical Materials Research 2000, 52, 577-586.

(129) Ito, Y.; Inaba, M.; Chung, D.; Imanishi, Y.; Control of Water Permeation by pH and ionic strength through a porous membrane having poly(carboxylic acid) surface-grafted. Macro molecules 1992, 25, 7313–7316.

(130) Nguyen, C. V; Delzeit, L.; Cassell, A. M.; Li, J.; Han, J.; Meyyappan, M.; Preparation of Nucleic Acid Functionalized Carbon Nanotube Arrays. Nano Letters 2002, 2, 1079-1081.

(131) Hinds, B. J.; Chopra, N.; Rantell, T.; Andrews, R.; Gavalas, V.; Bachas, L. G.; Aligned Multiwalled Carbon Nanotube Membranes. Science 2004, 303, 62–65.

(132) Krishnakumar, P.; Tiwari, P. B.; Staples, S.; Luo, T.; Darici, Y.; He, J.; Lindsay, S. M.; Mass Transport Through Vertically Aligned Large Diameter MWCNTs Embedded in Parylene. Nanotechnology 2012, 23, 455101.

(133) Nednoor, P.; Chopra, N.; Gavalas, V.; Bachas, L. G.; Hinds, B. J.; Reversible Biochemical Switching of Ionic Transport Through Aligned Carbon Nanotube Membranes. Chemistry of Materials 2005, 17, 3595–3599.

(134) Majumder, M.; Chopra, N.; Hinds, B. J.; Mass Transport Through Carbon Nanotube Membranes in Three Different Regimes: Ionic Diffusion and Gas and Liquid Flow. ACS nano 2011, 5, 3867–3877.

(135) Majumder, M.; Chopra, N.; Hinds, B. J.; Effect of Tip Functionalization on Transport Through Vertically Oriented Carbon Nanotube Membranes. Journal of the American Chemical Society 2005, 127, 9062–9070.

(136) Mazloumi, M.; Shadmehr, S.; Rangom, Y.; Nazar, L. F.; Tang, X. S.; Fabrication of Three-dimensional Carbon Nanotube and Metal Oxide Hybrid Mesoporous Architectures. ACS nano 2013, 7, 4281–4288.

(137) Sears, K.; Dumée, L.; Schütz, J.; She, M.; Huynh, C.; Hawkins, S.; Duke, M.; Gray, S.; Recent Developments in Carbon Nanotube Membranes for Water Purification and Gas Separation. Materials 2010, 3, 127–149.

(138) Hinds, B.; Aligned Multiwalled Carbon Nanotube Membranes. Current Opinion in Solid State and Materials Science 2012, 16, 1–9.

(139) Tawfick, S.; De Volder, M.; Hart, a J.; Structurally Programmed Capillary Folding of Carbon Nanotube Assemblies. Langmuir : the ACS journal of surfaces and colloids 2011, 27, 6389–6394.